Jian, Qian

CLOSURE PROBLEM AND NUMERICAL STUDIES OF TURBULENCE

City University of New York PH.D. 1984

CLOSURE PROBLEM AND NUMERICAL STUDIES OF TURBULENCE

by

Qian Jian

A dissertation submitted to the Graduate Faculty in Engineering in partial fulfillment of the requirements for the degree of Doctor of Philosophy, The City University of New York

1984

This manuscript has been read and accepted for the Graduate Faculty in Engineering in satisfaction of the dissertation requirement for the degree of Doctor of Philosophy.

April 4, 1984
date

Chan Mou Tchen
Chairman of Examining Committee

April 4, 1984
date

Paul R. Kaymal
Executive Officer

Supervisory Committee:

Professor W. J. Pierson

Professor C. M. Tchen
(Mentor and Chairman)

Professor N. Tzoar

Professor R. L. Varley

Professor L. Weinberg

The City University of New York

Abstract

CLOSURE PROBLEM AND NUMERICAL STUDIES OF TURBULENCE

by

Qian Jian

Adviser: Professor Chan Mou Tchen

A variational approach is proposed to solve the closure problem of turbulence theory and to derive the Kolmogorov law in an Eulerian framework. Two convergent integral equations are obtained for two unknown functions. The Kolmogorov constant Ko is evaluated numerically, obtaining Ko=1.2, which is compatible with the experimental data.

The initial-value problem of a forced Burgers equation is numerically solved by the Fourier expansion method. It is found that its solutions finally reach a steady state of 'laminar flow' which has no randomness and is stable to disturbances. Hence, strictly speaking, the so-called Burgers turbulence is not a turbulence. A new one-dimensional model of turbulence is proposed to simulate the Navier-Stokes turbulence. A series of numerical experiments on this one-dimensional turbulence are made and successful in obtaining Kolmogorov's $k^{-5/3}$ inertial-range spectrum. The (one-dimensional) Kolmogorov constant ranges from 0.5 to 0.65.

Finally the variational approach proposed in the first

part of this research is applied to the new one-dimensional model of turbulence proposed in the second part. The Kolmogorov's inertial-range law is derived analytically, the corresponding theoretical (one-dimensional) Kolmogorov constant is o.55, which is in good agreement with the results of the numerical experiments on the one-dimensional turbulence.

ACKNOWLEDGEMENTS

The author would like to express his appreciation to Professor C. M. Tchen for his guidance and encouragement.

The author is grateful to Deans Professor David H. Cheng and Professor Paul R. Karmel for their support.

The author wishes to thank Professor P. Ganatos who has given him much help in using computer. He also wishes to thank many members of the Faculty of The City University of New York who have taught him or given him help.

Table of Contents

LIST OF TABLES

LIST OF FIGURES

INTRODUCTION

Turbulence abounds in nature. In fact, turbulence plays a vital part in the dynamics of the widest variety of fluid motions on scales from millimeters to light years. In a turbulent flow, mass, momentum and energy transport rate greatly exceed the corresponding molecular transport rate. The important characteristics of turbulent flows are their apparent randomness and instability to small disturbances. Although the dynamic state of the fully-developed turbulence is extremely sensitive to triggering disturbances, the statistically average properties are not. On the other hand, transition flows have statistical properties which are sensitive to the nature of disturbances. In turbulence theory, the turbulence is generally understood to be fully-developed, so turbulence is a random flow field which are extremely sensitive to small disturbances, but has statistical properties which are not sensitive to disturbances.

The evolution of dynamic states of a turbulence is described by the Navier-Stokes equations. In a sense, the turbulence theory deals with the statistical solutions of the Navier-Stokes equations, which are nonlinear and equivalent to an infinite hierarchy of equations coupling together all the moments of the random velocity fields. Any finite subset of the infinite hierarchy of equations is not closed, and possesses more unknowns than are determined by the subset. The central problem of turbulence theory is to find proper approximation methods of converting the infinite

hierarchy of equations into a closed subset, that is the 'closure problem'[1-4].

One well-known historical approach to the closure problem is the cumulant-discard approximation[1,4]. When we keep the first, second and third-order cumulants but neglect the forth-order cumulant, it is equivalent to assume that the quadruple and the pair correlations are related as they would be if the probability distribution was Gaussian. So it is also called quasi-normal approximation. The quasi-normal approximation is now completely discredited because it gives negative energy spectra[5]. The physical reason for its disqualification is its total neglect of the most important dynamic damping effect due to the nonlinear interaction between different modes.

Kraichnan[6-14] developed a direct-interaction (DI) approximation to solve the closure problem and to take account of the dynamic damping effect of the nonlinear interaction, obtaining two integral equations for two unknown functions: the energy equation and the response equation. In an Eulerian framework, the response equation is divergent at zero wavenumber, and the $k^{-3/2}$ inertial-range spectrum obtained, instead of Kolmogorov's $k^{-5/3}$ spectrum, which is supported by experiments. Kraichnan identified the use of an Eulerian framework as the cause of this divergence, developed further the DI approximation in a Lagrangian formulation. Its mathematics is complicated, because the work is done in a Lagrangian framework. Kraichnan proposed the test-field model

(TFM), which is mathematically simpler and consistent with the Kolmogorov law. Unfortunately there is an artificial adjustable parameter in the TFM to make the result of TFM agree with experiments. Hence the TFM is a semi-empirical theory.

Edwards[15,16] and Herring[17] proposed the Fokker-Planck method and self-consistent field method respectively, and obtained the same energy equation as Kraichnan. Several forms of response equation of the F-P method have been suggested, but they are all divergent at zero wavenumber[1]. Later Edwards and McComb[16] argued that the energy equation is an expression of the principle of conservation of energy and the response equation should be derived as the expression of another physical principle, and developed the entropy method to solve the closure problem. They applied the principle of maximum entropy to a stationary turbulence, and succeeded in getting a Kolmogorov-type inertial-range spectrum in an Eulerian framework, but gave rather poor value of Kolmogorov constant. Moreover the applicability of the principle of the maximum entropy to turbulence is questionable.

Tchen[18,19] developed a kinetic approach to the closure problem. By using a Liouville-type equation in phase space, Tchen derived a kinetic equation for the probability distribution of velocity and a transition equation for the probability distribution of paths, forming two master equations consistent with the Navier-Stokes equations. The closure is obtained by the scaling procedure which distinguishes three basic processes: macro-evolution, micro-transport and sub-

micro-relaxation. Memory is present as a consequence of the non-markovian processes, leading to tensor-type viscosity and diffusivity instead of scalar ones. The memory-chain is cut off by requiring the relaxation process for transport properties to approach equilibrium. A scaled energy equation is derived and the energy spectrum is obtained directly due to the scaling procedure, yielding Kolmogorov's inertial-range spectrum. It is an elegant physical approach to the closure problem of turbulence. Any approach to the closure problem must contain some key approximation which have to be justified. In Kraichnan's theory it is the DI approximation, in Tchen's kinetic theory it is the scaling procedure and the physical assumptions about the three basic processes of turbulence.

CHAPTER I. VARIATIONAL APPROACH TO CLOSURE PROBLEM

A variational approach is proposed to solve the closure problem and to derive Kolmogorov law in an Eulerian frame. Like Edwards' Fokker-Planck method[15,16] and Tchen's kinetic method[18,19], probability distribution in phase space and Liouville equation are introduced. In Tchen's kinetic method the probability distribution of velocity is used and then a Fourier transform is made so that energy spectrum is obtained by a scaling procedure. In the proposed variational approach the Fourier transform is made at the beginning and the probability distribution of modal parameters is used, therefore the energy spectrum can be obtained without appealing to the scaling procedure.

Instead of using complex Fourier components of velocity as modal parameters as done in Edwards and Herring's formalism, a complete set of independent real parameters and its dynamic equations are worked out to describe the modal dynamics of a turbulence. An approximate solution of the stationary Liouville equation is obtained by a perturbation method, based upon a Langevin-Fokker-Planck (LFP) model.

The error of the perturbation solution depends on the error of the LFP model, which is expressed as a functional of the dynamic damping coefficient η. The functional assume the form of mean-square error according to the optimum-parameter-estimation method. The η will be treated as

an optimum control parameter to minimize the error of the perturbation solution. By a variational method we obtain a convergent integral equation for the optimum η, which will be used to replace the divergent response equation of Kraichnan's DI approximation. The energy equation and this convergent integral equation form a closed set of equations for two unknowns, solving the closure problem in a pure Eulerian framework. This closed set of equations will be used as basis for study of the statistical properties of turbulence.

Finally the Kolmogorov law is derived and the Kolmogorov constant is numerically evaluated, obtaining Ko=1.2, which is compatible with the experimental data.

1.1. Modal parameters and modal dynamic equations

For simplicity of mathematics, a homogeneous incompressible turbulence is supposed to be confined within a large cubic box with sides L and cyclic boundary conditions. The L will be let to approach infinity later. The Fourier transform of Navier-Stokes equations is[1]

$$(\frac{d}{dt} + \nu k^2)u_i(\underline{k}) = -i\frac{H}{2}(k_m P_{ij}(\underline{k})+k_j P_{im}(\underline{k})) \times \sum_{\underline{p},\underline{r}} u_j(\underline{p})u_m(\underline{r})\delta_{\underline{k},\underline{p}+\underline{r}} \quad , \tag{1.1}$$

where ν is kinematic viscosity, $H=(2\pi/L)^3$, $\delta_{\underline{k},\underline{p}+\underline{r}}$ is the Kronecker symbol; $\underline{k},\underline{p},\underline{r}$ are discrete wavevectors,

$$u_i(\underline{k}) = (2\pi)^{-3} \int_{box} u_i(\underline{x})\exp(-i\underline{k}\cdot\underline{x})\, d\underline{x} \tag{1.2}$$

are the Fourier transform of velocity components $u_i(\underline{x})$, and

$$P_{ij}(\underline{k}) = \delta_{ij} - k_i k_j / k^2 \tag{1.3}$$

is the projector operator. Due to incompressibility and $u_i(\underline{x})$being real quantities, $u_i(\underline{k})$are not independent, and

$$k_i u_i(\underline{k}) = 0 \ , \quad u_i(\underline{k}) = u_i^*(-\underline{k}) \ . \tag{1.4}$$

The asterisk means complex conjugate. The complex Fourier components $u_i(\underline{k})$ and $u(-\underline{k})$are often used as modal parameters by some authors[15-17], similar to the notations used in quantum field theory. In order to preserve a clear physical

meaning of the probability distribution in phase space in the frame of classical statistical mechanics, a complete set of independent real modal parameters and its dynamic equations are worked out in Appendix A to describe the modal dynamics of turbulence. The resulting modal dynamic equations are

$$(\frac{d}{dt}+\nu_i)X_i = \sum_{j,m} A_{ijm}X_jX_m \quad , \tag{1.5}$$

$\nu_i=\nu k^2$. Here, and afterwards, the Einstein summation convention is not used for indexes i,j,m, which are the combination of wavevector, component index and real-imaginary- part index. Do not confuse them with those in (1.1)-(1.4). The (X_i, $i\geq 0$) form a complete set of independent real modal parameters.

$$A_{ijm} = M_{ijm}+M_{ij-m}+M_{i-jm}+M_{i-j-m} \quad , \tag{1.6}$$

$$M_{ijm} = HS(i)S(j)S(m)P_{abc}(\underline{k},\underline{p},\underline{r})C^{\alpha\beta\gamma}\delta_{\underline{k},\underline{p}+\underline{r}} \quad . \tag{1.7}$$

For further information see Appendix A. It is indispensable for actual calculation to find a particular set of modal parameters and the explicit expression for A_{ijm}.

For the study of high-wavenumber-range dynamics, the model of stationary turbulence is assumed. Actually space homogeneity and time stationarity are conflict conditions for any turbulent flow, a homogeneous turbulence is at the same time a decaying turbulence[2,3]. The trick to solve this conflict is to assume that some external driving force is con-

tinuously supplying energy to the turbulence at low wavenumber to prevent it from decaying. The particular structure of this force is not relevant, for simplicity, supposing that it has form $\gamma_i' X_i$. Hence the modal dynamic equation (1.5) becomes

$$\frac{d}{dt}X_i = -(\gamma_i - \gamma_i')X_i + \sum_{j,m} A_{ijm} X_j X_m \quad . \tag{1.8}$$

Since γ_i' is different from zero only at low wavenumber, at later stage of analysis of the high-wavenumber range, it can be omitted.

1.2. Liouville equation

By classical statistical mechanics, all possible dynamic states of the turbulence, or all possible sets $(X_i, i\geq 0)$, constitute a phase space, which is called modal phase space to emphasize the difference between turbulence and a canonical system. The statistical behavior of the turbulence is described by the probability distribution over an ensemble of numerous realizations of the turbulence, denoted by $P = P(X_i, i\geq 0)$.

The evolution of the probability distribution satisfies the following Liouville equation

$$\frac{\partial P}{\partial t} + \bar{L}P = 0 \quad , \tag{1.9}$$

where $\bar{L}$ is the Liouville operator. Its structure is determined by the modal dynamic equation (1.8), and[1]

$$\bar{L} = -\sum_i \Big((\nu_i - \nu_i')\frac{\partial}{\partial X_i} X_i - \sum_{j,m} A_{ijm} X_j X_m \frac{\partial}{\partial X_i} \Big) \quad . \tag{1.10}$$

The Liouville equation (1.9) is linear, although its corresponding modal dynamic equation (1.8) are not linear. Notice that the summation over indexes i,j,m in Eqs. (1.5) (1.8) and (1.10) are restricted to be over their nonnegative values.

1.3. Langevin-Fokker-Planck (LFP) model

The terms on the right side of (1.8) represent the forces acting on mode i. The second term is the nonlinear interaction force, acting on mode i by all other modes in a mode sea. Its simplified mode is[9,15,17]

$$\sum_{j,m} A_{ijm} X_j X_m \simeq -\zeta_i X_i + f_i \ , \tag{1.11}$$

here $-\zeta_i X_i$ is the dynamic damping force and is deterministic for the mode i, represent the average effect of nonlinear interaction on mode i; f_i is a random force of the type of white noise. From (1.8) and (1.11) we have

$$\frac{d}{dt} X_i \simeq -\eta_i X_i + f_i \ , \quad \eta_i = \zeta_i + (\nu_i - \nu_i') \ . \tag{1.12}$$

For the high-wavenumber-range $\nu_i'=0$, we have

$$\eta_i = \zeta_i + \nu_i \ . \tag{1.13}$$

Eq. (1.12) is the Langevin equation, its Liouville equation is the Fokker-Planck equation, and its corresponding Liouville operator is the Fokker-Planck operator[20]

$$\bar{L}^{(f)} = -\sum_i \eta_i \left(\frac{\partial}{\partial X_i} X_i + \phi_i \frac{\partial^2}{\partial X_i^2} \right) \ , \tag{1.14}$$

here ϕ_i are related to the random force f_i in (1.11). Hence the simplified model (1.11) implies that the exact Liouville operator (1.10) can be approximated by the Fokker-Planck operator (1.14)

$$\bar{L} \simeq \bar{L}^{(f)} \ . \tag{1.15}$$

1.4. Perturbation solution

For a stationary turbulence the Liouville equation can be written as follows

$$(\bar{L}^{(f)} + (\bar{L} - \bar{L}^{(f)}))P = 0 \ . \tag{1.16}$$

According to the LFP model (1.11)-(1.15) $\delta\bar{L}=(\bar{L}-\bar{L}^{(f)})$ can be considered a small perturbation operator. Hence the approximate solution of (1.16) at zero order, denoted by $P^{(0)}$, satisfies the following equation,

$$\bar{L}^{(f)} \, P^{(0)} = 0 \ . \tag{1.17}$$

Eq. (1.17) is Fokker-Planck equation, its solution is Gaussian density function[1,15]

$$P^{(0)} = \prod_i (2\pi\phi_i)^{-1/2} \exp(-X_i^2 / (2\phi_i)) \ . \tag{1.18}$$

Let

$$P = P^{(0)} + P^{(1)} \ . \tag{1.19}$$

Since $\delta\bar{L}=(\bar{L}-\bar{L}^{(f)})$ is a small perturbation operator, $P^{(1)}$ is also small, substituting (1.19) into (1.16), using (1.17) and neglecting product term of $\delta\bar{L}$ and $P^{(1)}$, we have

$$\bar{L}^{(f)} \, P^{(1)} = -\delta\bar{L} \, P^{(0)} = -\bar{L} \, P^{(0)} \ . \tag{1.20}$$

From (1.10) and (1.18), Eq. (1.20) becomes

$$\bar{L}^{(f)} P^{(1)} = \Big(\sum_i (\nu_i - \nu_i')(1 - X_i^2/\phi_i) + \sum_{ijm} A_{ijm} X_i X_j X_m / \phi_i \Big) P^{(0)} \ . \tag{1.21}$$

By using the following equations

$$\bar{L}^{(f)} X_i P^{(0)} = \eta_i X_i P^{(0)}, \quad \bar{L}^{(f)} (X_i^2 - \phi_i) P^{(0)} = 2\eta_i (X_i^2 - \phi_i) P^{(0)}, \tag{1.22}$$

we solve Eq.(1.21) to get $P^{(1)}$. Then substitute it into (1.19), finally we have

$$P = \Big(1 - \sum_i (\gamma_i - \gamma_i') \frac{X_i^2 - \phi_i}{2 \eta_i \phi_i} + \sum_{ijm} \frac{A_{ijm} X_i X_j X_m}{\phi_i (\eta_i + \eta_j + \eta_m)} \Big) P^{(0)}, \tag{1.23}$$

A similar form of (1.23) was derived by Edwards in a different formulation[15,16]. The probability distribution (1.23) satisfies the normality condition,

$$\int P \prod dX_i = 1 \quad . \tag{1.24}$$

1.5. Energy equation

Using the Liouville equation (1.9) and (1.10), we have

$$\frac{d}{dt}\langle X_i^2\rangle = \int X_i^2(\frac{\partial}{\partial t}P)\prod dX_n = -\int X_i^2 \bar{L}P\prod dX_n$$

$$= -2(\nu_i-\nu_i')\langle X_i^2\rangle + 2\sum_{j,m}' A_{ijm}\langle X_i X_j X_m\rangle \quad . \tag{1.25}$$

The last step is based upon an integration by parts. By the probability distribution (1.23), the average modal intensity

$$\langle X_i^2\rangle = \int X_i^2 P\prod dX_n = e_i\phi_i \quad , \tag{1.26a}$$

$$e_i = 1 - (\nu_i-\nu_i')/\eta_i \quad . \tag{1.26b}$$

In the high-wavenumber-range, $\nu_i'=0$, so

$$e_i = 1 - \nu_i/\eta_i = \varepsilon_i/\eta_i \quad . \tag{1.27}$$

For isotropic turbulence, $\langle X_i^2\rangle$, e_i, η_i and ε_i are functions of k only, and

$$e(k) = \varepsilon(k)/\eta(k) \quad , \quad \eta(k) = \varepsilon(k) + \nu k^2 \quad . \tag{1.28}$$

From (1.23) and (1.26), the triple correlation of modes

$$\langle X_i X_j X_m\rangle = \int X_i X_j X_m P\prod dX_n = 2B_{ijm}/(\eta_i+\eta_j+\eta_m) \quad , \tag{1.29}$$

$$B_{ijm} = A_{ijm}\phi_j\phi_m + A_{jmi}\phi_m\phi_i + A_{mij}\phi_i\phi_j \quad . \tag{1.30}$$

Let

$$E(k) = 4\pi k^2 q(k) \tag{1.31}$$

be the three-dimensional energy spectrum, it can be proved that[1]

$$q(k) = 2H\langle x_i^2 \rangle \quad , \quad H = (2\pi/L)^3 \ . \tag{1.32}$$

For the study of high-wavenumber-range, the ν_i' is omitted. Let L, the size of the cubic box introduced at the beginning of Section 1.1, approach infinity, from (1.25)-(1.32) and the formula in Appendix B, after long manipulation, Eq. (1.25) becomes

$$(\frac{d}{dt} + 2\nu k^2)E(k) = T(k) \ , \tag{1.33}$$

$$T(k) = 16\pi^2 \iint_{\Delta} dpdr \ \frac{k^3 prb(k,p,r)\ \tilde{q}(r)\ [\tilde{q}(p) - \tilde{q}(k)]}{\eta(k) + \eta(p) + \eta(r)} \ ,$$

$$q(k) = e(k)\tilde{q}(k) \ . \tag{1.34}$$

Here b(k,p,r) is a geometrical factor defined by (B.11) in Appendix B. T(k) is the energy transfer spectrum function.

1.6. Variational approach

The energy equation (1.33)-(1.34) contains two unknown functions: the energy spectrum q (or E) and the dynamic damping coefficient η. Another equation for q and η is needed to solve the closure problem.

The validity and error of the perturbation solution (1.23) depends on the validity and error of the LFP model (1.11)-(1.15). There are two adjustable parameters η and ϕ in the LFP model. Due to Eq. (1.26), the actual adjustable parameter is η. The LFP model can be made as good as possible by choosing the optimum η which minimizes the error of the LFP model.

An appropriate measure of the error of the LFP model is expressed as an functional of η, denoted by $I=I(\eta)$. By variational method[21], the optimum η, which minimizes I, satisfies

$$\frac{\delta I}{\delta \eta} = 0 \quad . \tag{1.35}$$

Eq. (1.35) will lead to a convergent integral equation for q and η to replace the divergent response equation of Kraichnan's DI approximation, thus solving the closure problem in an Eulerian framework and at the same time making the error of the perturbation solution (1.23) as small as possible in the frame of the LFP model.

Actually $\eta=(\eta_i, i\geq 0)$ is a vector of infinity dimension in the preceding formulation, so (1.35) is equivalent to

$$\frac{\partial I}{\partial \eta_i} = 0 \quad . \tag{1.36}$$

1.7. Mean-square estimation of η

The success of the variational approach depends on the proper choice of the functional $I=I(\eta)$, which expresses the error of the LFP model. The mean-square error of optimum-parameter-estimation for a stochastic process is to be used to define the functional I.

The LFP model is based on the approximation (1.11), which can be interpreted as follows: a simple model of stochastic process $-\zeta_i X_i+f_i$ is used to approximate a complicated actual process on the left side of (1.11). the model process is a linear transform of a given stochastic process X_i superposed by a white noise f_i. The coefficients of the linear transform, ζ_i or η_i, is to be adjusted so that the model process will approximate the actual process as well as possible. This is the typical formulation of optimum-parameter-estimation problems in control theory[22,23]. The usual approach is the mean-square estimation method, i.e., the 'optimum' is interpreted in the mean-square sense. Hence

$$I = \sum_i \left\langle \left(\sum_{j,m} A_{ijm} X_j X_m - (-\zeta_i X_i) \right)^2 \right\rangle , \qquad (1.37)$$

Here $\langle \ldots \rangle$ means ensemble average.

Making use of (1.13),(1.23),(1.26),(1.29) and (1.30) we obtain

$$\zeta_i \langle X_i^2 \rangle = 2 \sum_{j,m} \left(\frac{C_{ijm} B_{ijm}}{\eta_{ijm}^2} - \frac{A_{ijm} B_{ijm}}{\eta_{ijm}} - \frac{\nu_i}{\eta_i^2} \langle X_j^2 \rangle \langle X_m^2 \rangle \frac{A_{ijm} C_{ijm}}{\eta_{ijm}} \right). \qquad (1.38a)$$

Here

$$C_{ijm} = A_{ijm}\zeta_i + A_{jim}\zeta_j + A_{mij}\zeta_m \quad , \tag{1.38b}$$

$$\eta_{ijm} = \eta_i + \eta_j + \eta_m \quad . \tag{1.38c}$$

Let L approach infinity. Similar to the derivation from (1.25) to (1.33)-(1.34), from (1.38) we have

$$\eta(k) = \nu k^2 + \frac{2\pi}{q(k)} \iint_{\Delta} dpdr \, \frac{kpr}{(\eta(k,p,r))^2} \Big[b(k,p,r)d(r,p,k) \times \big(\eta(k,p,r) - \zeta(k) + \zeta(p)\big) + \overset{*}{b}(k,p,r)d(k,p,r)\zeta(p) + \frac{\nu k^2 \eta(k,p,r)}{(\ (k))^2} q(k)q(r) \Big(b(k,p,r)(\zeta(p)-\zeta(k)) + \overset{*}{b}(k,p,r)(\zeta(p)-\zeta(r)) \Big) \Big] . \tag{1.39a}$$

Here

$$\eta(k,p,r) = \eta(k) + \eta(p) + \eta(r) \quad , \tag{1.39b}$$

$$d(k,p,r) = \tilde{q}(k)\big(\tilde{q}(r) - \tilde{q}(p)\big) \tag{1.39c}$$

and

$$\overset{*}{b}(k,p,r) = \frac{pr}{k^2}(yz + x^3) \quad . \tag{1.39d}$$

The x,y,z are cosines of three angles of the triangle with sides k, p and r (see Appendix B).

The energy equation (1.33) with (1.34) and the η equation (1.39) form a closed set of equations for two unknown functions q (or ϕ) and η. In principle, by using the probability (1.23) and the closed set of equations for q (or ϕ) and η, we can calculated the statistical properties of turbulence. As an example we apply them to study the inertial-range and to derive the Kolmogorov law.

1.8. Energy equation and η equation for inertial-range

In the inertial-range the viscous dissipation is negligible, $\nu k^2=0$, from (1.28) we have

$$\zeta(k) = \eta(k) , \qquad e(k) = 1 . \tag{1.40}$$

Hence (1.34) becomes

$$T(k) = 16\pi^2 \iint^{\Delta} dpdr\ k^3pr \frac{b(k,p,r)q(r)(q(p)-q(k))}{\eta(k)+\eta(p)+\eta(r)} . \tag{1.41}$$

T(k) is the energy transfer spectrum function. The energy transfer function

$$\Pi(k) = \int_k^{\infty} T(k')dK' \tag{1.42}$$

is the energy flow rate across the spectrum. Due to Kraichnan[1], it has the following convenient expression:

$$\Pi(k) = \int_k^{\infty} dk' \int_0^k dp \int_{p^*}^{p+k'} dr\ S(k'|p,r) , \tag{1.43a}$$

$$p^* = \max(p,\ k'-p) , \tag{1.43b}$$

$$S(k|p,r) = \frac{16\pi^2k^3pr}{\eta(k)+\eta(p)+\eta(r)} \left[b(k,p,r)q(r)(q(p)-q(k)) + b(k,r,p)q(p)(q(r)-q(k))\right] . \tag{1.43c}$$

In the inertial-range, the energy transfer function $\Pi(k)$ is independent of k and is equal to the dissipation

rate of energy $\epsilon = 2\int_o^\infty \nu k^2 E(k)dk$, therefore

$$\epsilon = \int_k^\infty dk' \int_0^k dp \int_{p^*}^{p+k'} dr \; S(k'|p,r) \quad . \qquad (1.44)$$

In the inertial-range $\nu k^2 = 0$, so $\eta(k) = \zeta(k)$ and $e(k) = 1$, Eq. (1.39) becomes

$$\eta(k) = \frac{2\pi}{q(k)} \iint_\Delta dpdr \; \frac{kpr}{(\eta(k)+\eta(p)+\eta(r))^2} \Big[b(k,p,r)q(r) \times (q(k)-q(p))(2\eta(p)+\eta(r)) + b^*(k,p,r)q(k) \times (q(r)-q(p))\eta(p) \Big] \quad . \qquad (1.45)$$

The energy equation (1.44) and the η equation (1.45) constitute a closed set of integral equations for $q(k)$ and $\eta(k)$ in the inertial-range.

1.9. Kolmogorov law and Kolmogorov constant

The idealized model of inertial-range dynamics of a turbulence is: an energy source is at zero wavenumber and an energy sink is at infinite wavenumber, with a energy flow across the spectrum at the constant rate ϵ. Eqs. (1.44) and (1.45) form a closed set of equations for two unknowns q(k) and $\eta(k)$. Supposing that q(k) and $\eta(k)$ have the form of power function,

$$q(k) = C_q k^m \quad , \qquad \eta(k) = C_\eta k^n \quad . \tag{1.46}$$

Substitute (1.46) into (1.44) and (1.45), we obtain

$$5 + m - 2n = 0 \quad , \qquad 8 + 2m - n = 0 \quad . \tag{1.47}$$

Hence m=-11/3 and n=2/3. Let $C_q=(Ko/4\pi)\epsilon^{2/3}$ and $C_\eta=D\epsilon^{1/3}$, (1.46) becomes

$$q(k) = (Ko/4\pi)\epsilon^{2/3}k^{-11/3} \quad , \tag{1.48}$$

$$\eta(k) = D\epsilon^{1/3}k^{2/3} \quad . \tag{1.49}$$

From (1.31) and (1.48) we have

$$E(k) = Ko\ \epsilon^{2/3}\ k^{-5/3} \quad , \tag{1.50}$$

which is the Kolmogorov inertial-range law. We are successful in deriving Kolmogorov law from the first principle of statistical mechanics.

Substitute (1.48) and (1.49) into (1.44) and (1.45), then calculating the two resulting double integrals by

numerical method, we obtain

$$D/Ko^2 = 0.19 \ , \quad D^2/Ko = 0.0605 \ . \tag{1.51}$$

The D/Ko^2 is first evaluated by Kraichnan[1]. From (1.51) the Kolomogorov constant is

$$Ko \simeq 1.2 \ . \tag{1.52}$$

The experimental value of Kolmogorov constant given by Gibson and Schwarz[24] is 1.28–1.32. At the present stage of experimental and theoretical research on turbulence, it is unrealistic to require a turbulence theory to reproduce the experimental data accurately to more than two digits. In this sense, the Kolmogorov constant given by (1.52) is compatible with the experimental data quite well.

CHAPTER II. NUMERICAL EXPERIMENTS ON ONE-DIMENSIONAL MODEL OF TURBULENCE

The difficulties of the problem of turbulence are of twofold nature: in part they are connected with the complicated vectorial character of the Navier-Stokes equation; in part they are dependent upon the presence of nonlinear term. The later feature is essential for turbulence, a linear dynamic equation cannot generate 'turbulence' solution. Burgers proposed the equation[25]

$$\frac{\partial}{\partial t}u(t,x) + u(t,x)\frac{\partial}{\partial x}u(t,x) = \nu\frac{\partial^2}{\partial x^2}u(t,x) \qquad (2.1)$$

as an one-dimensional analogy of the Navier-Stokes equation in order to simplify the problem of turbulence by avoiding its complicated vectorial character.

At present we can not numerically simulate the flow field at sufficiently high Reynolds number to produce the inertial-range in two- or three-dimensional flow, because of insufficient computer capacity[26-28]. An one-dimensional model is needed. The commonly-used model is Burgers equation or its forced form, the so-called Burgers turbulence. The solution of Eq.(2.1) can be expressed in terms of initial data and such a turbulence (without external force) has been studied by many authors[29-34]. The numerical experiments dealing with an external force was made by Jeng[35] for small viscosity and by Kida and Sugihara[36] for the inviscid limit.

All the analytic and numerical studies lead to the conclusion that the k^{-2} inertial-range spectrum is the characteristic feature of Burgers turbulence. In contrast, for Navier-Stokes turbulence the cascade transfer of energy from large eddies to small eddies yields the Kolmogorov's $k^{-5/3}$ inertial-range spectrum. That is related to the essential difference between Burgers equation and Navier-Stokes equation, and indicates that the Burgers equation is not a proper one-dimensional model of the Navier-Stokes turbulence[37].

First of all the Burgers equation with a steady external force acting at the lowest wavenumber is numerically integrated in order to study the long-time evolution of its solutions. The numerical results show that after sufficient long time these solutions reach a steady state of 'laminar flow', which has no randomness and is independent of the initial conditions, i.e., absolutely stable to disturbances. The essential characteristics of a turbulence are its randomness and instability to small disturbances. Hence, strictly speaking, the so-called Burgers turbulence is not a turbulence.

A new mathematical model is proposed as an one-dimensional analogy of the Navier-Stokes equation. It has a modified advection term and a pressure-type term. A series of numerical experiments on this one-dimensional model are made and are successful in obtaining the Kolmogorov's $k^{-5/3}$ inertial-range spectrum. The (one-dimensional) Kolmogorov constant ranges from 0.5 to 0.65.

Our numerical experiments confirm the vital role of the pressure term in hydrodyndmic turbulence. The nonlinear interaction of the advection term alone can not generate turbulence. The commonly-used one-dimensional model of turbulence (the Burgers turbulence) has a k^{-2} inertial-range spectrum. We are successful in proposing a one-dimensional model of the Navier-Stokes turbulence, which has a $k^{-5/3}$ inertial-range spectrum. The results of our numerical experiments will be used to test the validity and error of the variational approach to closure problem proposed in Chapter I.

2.1. Burgers equation and its Fourier transform

With a characteristic length L and a characteristic velocity V, by means of the dimensionless quantities $x'=x/L$, $t'=tV/L$ and $\nu'=\nu/(VL)$, (2.1) becomes

$$\frac{\partial}{\partial t'}u' + u'\frac{\partial}{\partial x'}u' = \nu'\frac{\partial^2}{\partial x'^2}u' \quad . \tag{2.2}$$

If we drop the primes in (2.2), (2.1) and (2.2) are identical. Hence (2.1) can be understood as the dimensionless form of Burgers equation, and ν is the reciprocal of Reynolds number. Afterwards all quantities and equations are assumed to be dimensionless.

Assuming the periodic boundary condition

$$u(t,x+2\pi) = u(t,x) \quad , \tag{2.3}$$

we can expand u(t,x) into the Fourier series

$$u(t,x) = \sum_k U(k)\exp(ikx) \quad , \tag{2.4}$$

where

$$U(k) = (1/2\pi)\int_0^{2\pi} u(t,x)\exp(-ikx)dx \tag{2.5}$$

is a function of time t. From (2.4), Burgers equation becomes

$$\frac{d}{dt}U(k) = -ikW(k) - \nu k^2 U(k) \quad , \tag{2.6}$$

and

$$W(k) = (1/2)\sum_p U(p)U(k-p) \tag{2.7}$$

by the convolution theorem.

If there is an external force, which is assumed to have the simple form $\mathcal{M}(k)U(k)$, (2.6) can be generalized as follows

$$\frac{d}{dt}U(k) = -ikW(k) + \mathcal{M}(k)U(k) - \mathcal{N}(k)U(k) \quad . \qquad (2.8)$$

Both $\mathcal{M}(k)$ and $\mathcal{N}(k)$ in (2.8) are positive, $\mathcal{M}(k)U(k)$ corresponds to the energy source and $\mathcal{N}(k)U(k)$ corresponds to the energy sink . When $\mathcal{M}(k)=0$ and $\mathcal{N}(k)=\nu k^2$, (2.8) becomes (2.6), and the energy sink is due to viscous dissipation.

The Fourier component U(k=0) represents the mean flow of the velocity field. From (2.6), we see that the mode k=0 has no interaction with other modes. For simplicity, we assume that U(k=0)=0, i.e., there is no mean flow.

2.2. Energy equation

The intensity of mode k is

$$\bar{e}(k) = U(k)U^*(k) \quad . \tag{2.9}$$

The asterisk means complex conjugate. From (2.8) we have

$$\frac{d}{dt}\bar{e}(k) = r(k) + 2\mathcal{U}(k)\bar{e}(k) - 2\mathcal{V}(k)\bar{e}(k) \quad , \tag{2.10}$$

here

$$r(k) = -ik(W(k)U^*(k) - W^*(k)U(k)) \quad . \tag{2.11}$$

From (2.7) and (2.11), it is easy to prove that

$$\sum r(k) = 0 \quad . \tag{2.12}$$

The total energy of all modes is

$$\sum_{k\geq 0}{}' \bar{e}(k) = (1/4\pi) \int_0^2 u^2(t,x)\, dx \quad . \tag{2.13}$$

The energy flow rate across the k space is

$$\bar{q}(k) = \sum_{k'>k}{}' r(k') = -\sum_{k'=1}^{k}{}' r(k') \quad . \tag{2.14}$$

In inertial-range $\mathcal{U}(k)=\mathcal{V}(k)=0$, From (2.10) and (1.14) we have $r(k)=0$ and $\bar{q}(k)$=constant for a steady state.

The ensemble average applied to (2.10) gives

$$\frac{d}{dt}E(k) = R(k) + 2\mathcal{U}(k)E(k) - 2\mathcal{V}(k)E(k) \quad , \tag{2.15}$$

here

$$E(k) = \langle\bar{e}(k)\rangle \tag{2.16}$$

is the energy spectrum, and

$$R(k) = \langle r(k) \rangle \tag{2.17}$$

is the energy transfer spectrum function; $\langle \ldots \rangle$ means ensemble average. The energy transfer function is

$$Q(k) = \langle \bar{q}(k) \rangle = \sum_{k'>k} R(k') = -\sum_{k'=1}^{k} R(k') \quad . \tag{2.18}$$

In inertial-range $\mathcal{M}(k)=\mathcal{N}(k)=0$. From (2.15) and (2.18) we have $R(k)=0$ and thus

$$Q(k) = \epsilon \text{ (constant)} \tag{2.19}$$

for stationary turbulence where ϵ represents the energy dissipation rate.

2.3. Inertial-range dynamics

The idealized model of inertial-range dynamics is that an energy source is at the lowest wavenumber and a sink is at infinite wavenumber, with an energy flow across the spectrum at a constant rate ϵ. It is impossible to work with an infinite wavenumber in a numerical experiment. The truncation approximation must be used, i.e., we assume

$$U(k) = 0 \quad \text{if } k > k_c \quad . \tag{2.20a}$$

Here the k_c is called cutoff wavenumber. The energy source is supposed to be acting at the lowest wavenumber k=1 only, i.e.,

$$\mathcal{M}(k) = 0 \quad \text{if } k > 1 \quad . \tag{2.20b}$$

The sink is supposed to be acting over the neighborhood of the cutoff wavenumber k_c only, i.e.,

$$\mathcal{N}(k) = 0 \quad \text{if } k \leqslant k_d \quad , \tag{2.20c}$$

where k_d is less than k_c but near k_c.

By (2.20) the generalized Burgers equation (2.8) becomes

$$\frac{d}{dt}U(1) = -iW(1) + \mathcal{M}(1)U(1) \quad , \tag{2.21a}$$

$$\frac{d}{dt}U(k) = -ikW(k) \quad \text{if } 2 \leqslant k \leqslant k_d \quad , \tag{2.21b}$$

$$\frac{d}{dt}U(k) = -ikW(k) - \mathcal{N}(k)U(k) \quad \text{if } k_d < k \leqslant k_c \quad . \tag{2.21c}$$

Eq. (2.21) describe the following process: the energy is

input at k=1, then is transfered to high wavenumbers by the nonlinear interaction W(k), finally is dissipated over the neighborhood of k_c. With the truncation approximation (2.20a), after some manipulation, (2.7) becomes

$$W(k) = \sum_{p=1}^{k_c-k} U(-p)U(k+p) + (1/2)\sum_{p=1}^{k-1} U(p)U(k-p) \quad , \qquad (2.22)$$

which will be used in numerical experiments.

2.4. Energy source and energy sink

Tentative numerical experiments of (2.21) show that when $\mu(1)$ in (2.21a) is too small the modal intensity $\bar{e}(k)$ decreases with time, when $\mu(1)$ is too large the $\bar{e}(k)$ increases with time, leading to overflow. It is more convenient to use a reservoir-type energy source which is able to adjust its input power automatically to keep the modal intensity $\bar{e}(1)$ constant. There are many ways to construct such an energy source. One way to do it is to replace (2.21a) by

$$\frac{d}{dt}U(1) = -iW(1) + C(|U_0(1)| - |U(1)|)U(1) \quad . \qquad (2.23)$$

Here C is a large positive amplification factor and $U_0(1)$ is the initial value of U(1). The $|...|$ means absolute value. The advection term -iW(1) in (2.23) transfers the energy from mode 1 to other modes and reduces the intensity of mode 1; the energy source represented by the last term in (2.23) inputs energy to mode 1 as soon as its intensity becomes less than the initial value, similar to a simple feedback system. An ideal reservoir-type energy source can balance the advection term -iW(1) exactly and keep U(1) a constant, i.e.,

$$\frac{d}{dt}U(1) = 0 \quad . \qquad (2.24)$$

In our numerical experiments the $\nu(k)$ in (2.21c) assumes the following form

$$\nu(k) = \nu_d(k-k_d)^n \quad . \tag{2.25}$$

Here ν_d and n are positive numbers. This structure of $\nu(k)$ makes the transition from the inertial-range to the dissipation-range a smooth one. Our numerical experiments show that the detailed structure of $\nu(k)$ does not influence the outcomes of the inertial-range dynamics, so long as the intensity of the energy sink matches the intensity of the energy source.

By (2.24) and (2.25), (2.21) becomes

$$\frac{d}{dt}U(1) = 0 \text{ or } U(1) = \text{constant} \quad , \tag{2.26a}$$

$$\frac{d}{dt}U(k) = -ikW(k) \quad \text{if } 2 \leqslant k \leqslant k_d \quad , \tag{2.26b}$$

$$\frac{d}{dt}U(k) = -ikW(k) - \nu_d(k-k_d)^n U(k) \quad \text{if } k_d < k \leqslant k_c \quad . \tag{2.26c}$$

When k_c and k_d approach infinity, (2.26) corresponds to the inviscid limit of the Burgers equation with an energy source at k=1 and energy sink at $k=\infty$.

The introduction of an energy source is indispensable for studying the long-time evolution of turbulence. If there is no energy source, the turbulence will decay and finally die out due to dissipation.

2.5. Numerical experiments of Eq. (2.26)

The Adams method is used to solve the initial-value problem of (2.26). The time step $\Delta t=0.005$ for $k_c=50$ and $\Delta t=0.0025$ for $k_c=100$ in order for the numerical process to be stable. Ten runs of such numerical experiments of (2.26) have been made on computer, corresponding to four different initial conditions, two cutoff wavenumbers and three types of energy sink. They are summed up in Table 2 and Fig. 1-4. The four initial conditions are

$$\begin{cases} U(1) = 1 & (2.27a) \\ U(k) = 0.3 \quad \text{if } 2 \leqslant k \leqslant 5 & (2.27b) \\ U(k) = 0.001 \quad \text{if } 6 \leqslant k \leqslant k_c \ , & (2.27c) \end{cases}$$

$$\begin{cases} U(1) = 1 & (2.28a) \\ U(k) = 0.31623 \quad \text{if } 2 \leqslant k \leqslant 5 & (2.28b) \\ U(k) = 0.001 \quad \text{if } 6 \leqslant k \leqslant k_c \ , & (2.28c) \end{cases}$$

$$\begin{cases} U(1) = 1 & (2.29a) \\ U(k) = 0.21 \quad \text{if } 2 \leqslant k \leqslant 10 & (2.29b) \\ U(k) = 0.001 \quad \text{if } 11 \leqslant k \leqslant k_c \ , & (2.29c) \end{cases}$$

$$\begin{cases} U(1) = \exp(i\pi/2) & (2.30a) \\ U(k) = 0.21\exp(i\pi k/2) \quad \text{if } 2 \leqslant k \leqslant 10 & (2.30b) \\ U(k) = 0.001\exp(i\pi k/2) \quad \text{if } 11 \leqslant k \leqslant k_c \ . & (2.30c) \end{cases}$$

The general behavior of the solutions of (2.26) is illustrated in Fig. 1 which is the result of run 1 (the actual numerical computation was done up to time t=15 instead of

t=6). Although Fig. 1 shows the time variation of the total energy only, the time variation of the intensity and phase of each mode have the same behavior. During the early stage the solutions of (2.26) undergo a transient process, the intensity of each mode except mode 1 varies with time rapidly. This transient process begins at t=0 and ends at t=4. After t=4 the solutions of (2.26) reach a steady state of 'larminar flow', which is characterized by the k^{-2} law for the modal intensity in the range $3<k<k_c/3$. See Fig. 1-4.

In the final steady state of 'laminar flow', the amplitude and phase of all modes are independent of time, so there is no randomness in the flow field at all. Moreover, the final steady state of 'laminar flow' is independent of the initial conditions, hence it is absolutely stable to disturbances. A comparison of Fig. 2 and 3 shows that in the final steady state of 'laminar flow' the behavior of the inertial-range ($3<k<k_c/3$) is independent of the structure of the energy sink, whose influence is limited to the neighborhood of the dissipation-range.

In the runs 1-6 k_c=50, in the runs 7-10 k_c=100. The increase of cutoff wavenumber k_c leads to the broadening of the inertial-range proportionally. It is logical to conclude that the general characteristics of the solutions of (2.26) will remain the same when k_c approach infinity and the inertial-range becomes infinitely wide, which corresponds to the inviscid limit of the Burgers turbulence with

an energy source at k=1 and an energy sink at k=∞. If we consider an ensemble of many realizations, corresponding to different initial conditions (and maybe different external forces at lower wavenumbers), the ensemble average will yield the well-known k^{-2} inertial-range spectrum for the so-called Burgers turbulence; since, according to our numerical experiments, the modal intensity of each realization is proportional to k^{-2} in the inertial-range after the transient process has ended.

2.6. Burgers turbulence is not a turbulence

The essential characteristics of a turbulence is its apparent randomness and instability to small disturbances. Two turbulent flows that are nearly identical in detail will appear dramatically different at later time, i.e., the extreme sensitivity of the solution of Navier-Stokes equation to the initial conditions. In the Burgers equation the only nonlinear term is the advection term, no pressure term. According to our numerical experiments described in Section 5, the nonlinear interaction of the advection term reduces the chaos of the flow field and builds correlation between modes, finally leads to a steady state of 'laminar flow' which is stable to disturbances. Contrary to the case of the Navier-Stokes equation, Burgers equation has solutions which are not random and are not sensitive to initial conditions. Hence, strictly speaking, the so-called Burgers turbulence is not a turbulence. The nonlinear interaction of advection alone cannot generate turbulence, no matter how high the Reynolds number is.

In the Navier-Stokes equation the pressure term plays the role of a high-frequency random force to limit the buildup of correlation between modes. The vortex structure in the flow field is not stable. The chaos of the flow field increases with time, finally leading to a state of turbulence which is random and unstable to small disturbances.

The essential difference between the Burgers equation and the Navier-Stokes equation lead to different inertial-range spectrum: k^{-2} for Burgers turbulence and $k^{-5/3}$ for the Navier-Stokes turbulence. The Burgers equation is not a proper one-dimensional model of the Navier-Stokes turbulence. A challenging problem logically arises: how to find a proper one-dimensional model of turbulence that has Kolmogorov's $k^{-5/3}$ inertial-range spectrum.

In the following we propose a new one-dimensional model of turbulence, which has a modified advection term and a pressure-type term. A series of numerical experiments on this one-dimensional turbulence is made, and is successful in obtaining Kolmogorov's $k^{-5/3}$ inertial-range spectrum.

2.7. One-dimensional model of Navier-Stokes turbulence

The proposed one-dimensional model is

$$\frac{d}{dt}U(k) = -ikW_m(k) + P(k) - \nu(k)U(k) \quad . \tag{2.31}$$

Here the $-ikW_m(k)$ is a modified advection term that transfers the energy from one mode to the others but conserves the total energy of all modes. The $P(k)$ is a pressure-type term to simulate the role of the pressure term of Navier-Stokes equation as a high-frequency conservative random force

As mentioned in Section 1.1., the Navier-Stokes equation can be transformed into the following form

$$\frac{d}{dt}X_i = -\nu_i X_i + \sum_{j,m} A_{ijm} X_j X_m \quad . \tag{2.32}$$

Here the $(X_i, i \geq 0)$ is the complete set of independent real modal parameters, and is related to the real and imaginary parts of the complex Fourier components of the turbulent velocity field. The remarkable property of the nonlinear interaction coefficients A_{ijm} is that

$$A_{ijm} = 0 \quad \text{if any two of } i,j,m \text{ are equal} \quad . \tag{2.33}$$

The property (2.33) is related to the incompressibility which requires the Fourier components of the velocity to be perpendicular to its wavenumber vector. However, when we transform the Burgers equation (2.6) into the form (2.32), the corresponding nonlinear interaction coefficients will

not satisfy (2.33) for no incompressibility condition. In order for the one-dimensional model (2.31) to simulate the Navier-Stokes equation as well as possible, the $W_m(k)$ in (2.31) is defined as follows

$$W_m(k) = W(k) - iU^{(2)}(2k)U^*(k) \quad \text{if } k \text{ is odd} \quad ; \tag{2.34a}$$

$$W_m(k) = W(k) - iU^{(2)}(2k)U^*(k) - 0.5(U^{(1)}(k/2))^2 + 0.5(U^{(2)}(k/2))^2 \quad \text{if } k \text{ is even} \quad . \tag{2.34b}$$

Here $W(k)$ is given by (2.7), the $U^{(1)}(k)$ and $U^{(2)}(k)$ are the real and imaginary parts of $U(k)$ respectively. We obtain (2.34) simply by discarding these terms in $W(k)$ that will not satisfy (2.33).

Similar to (2.10), the energy equation of the one-dimensional model (2.31) is

$$\frac{d}{dt}\bar{e}(k) = r_m(k)+U^*(k)P(k)+U(k)P^*(k)-2\nu(k)\bar{e}(k) \quad , \tag{2.35}$$

here

$$r_m(k) = -ik(W_m(k)U^*(k) - W_m^*(k)U(k)) \quad . \tag{2.36}$$

From (2.34) and (2.36), we have

$$\sum_k r_m(k) = 0 \quad . \tag{2.37}$$

Eq. (2.37) means that the nonlinear interaction term $-ikW_m(k)$ conserves the total energy of all modes.

The pressure term in the Navier-Stokes equation is a special 'isotropic' conservative force. It scarcely transfers the energy from lower wavenumbers to higher wavenumbers, but tends to equipartition the energy among all degrees of

freedom for the same wavenumber. In the 1-dimensional case, there are only two degrees of freedom for the same wavenumber, corresponding to the real and imaginary parts of U(k) respectively. In order for the term P(k) in (2.31) to simulate the pressure term of the Navier-Stokes equation as an 'isotropic' conservative force, it is required that

$$U^*(k)P(k) + U(k)P^*(k) = 0 \quad . \tag{2.38}$$

Let $\varphi(k)$ be the phase of mode k, i.e.,

$$\exp(i\varphi(k)) = U(k)/|U(k)| \quad , \tag{2.39}$$

then (2.38) means that

$$P(k) = \pm i|P(k)|\exp(i\varphi(k)) \quad . \tag{2.40}$$

If the intensity of all modes is amplified by the same factor C, the pressure term in the Navier-Stokes equation will be amplified by the same factor C also. Therefore we choose

$$P(k) = iA(k)|U(1)|^2\exp(i\varphi(k)) \quad . \tag{2.41}$$

Here A(k) is real (positive or negative). The pressure term in the Navier-Stokes equation plays the role of a random force to limit the buildup of correlation between modes, hence, we simply let A(k) to be random variables.

In numerical experiments the A(k) is simulated by uniformly-distributed pseudo-random numbers over the interval $(-a,a)$, based on the recurrent use of residues[38]

$$\alpha_{n+1} = \beta\alpha_n \pmod M \quad . \tag{2.42}$$

For example $\beta=7^9$ and $M=10^{10}$. In the numerical experiments, $a=2$, so the average amplitude of A(k) is equal to 1. The structure of A(k) will be described in detail later.

It has to be pointed out that the above reasoning and argument leading to the one-dimensional model (2.31) with (2.34) and (2.41) is plausible and rather arbitrary. The final justification of this mathematical model is that it is able to simulate the essential characteristics of the Navier-Stokes turbulence and yields a Kolmogorov's $k^{-5/3}$ inertial-range spectrum. We are not going to transform (2.31) into (t,x) space and give the resulting equation a specious 'physical meaning'. We prefer to work in the (t,k) space and consider our model (2.31) merely a mathematical (one-dimensional) model of turbulence.

2.8. Ensemble average and time average

According to Sections 2.3-2.4, for studying the inertial-range dynamics, (2.31) becomes

$$\frac{d}{dt}U(1) = i\omega U(1) \quad , \tag{2.43a}$$

$$\frac{d}{dt}U(k) = -ikW_m(k)+P(k) \quad 2 \leqslant k \leqslant k_d \quad , \tag{2.43b}$$

$$\frac{d}{dt}U(k) = -ikW_m(k)+P(k)-\nu_d(k-k_d)^n U(k) \quad k_d < k \leqslant k_c \quad . \tag{2.43c}$$

If $\omega=0$, (2.43a) is the same as (2.26a), then the energy source is identical with that described in the Section 2.4. The introduction of ω in (2.43a) is for the convenience of numerical computation. The energy transfer rate from mode 1 to mode 2, from mode 2 to mode 4, and so on, are quite sensitive to the phase of mode 1. In order to calculate the spectrum and other statistical properties of a turbulence by ensemble average, it is necessary to take account of all possible phases of mode 1. When using (2.26a) instead of (2.43a), we have to solve the initial-value problem of (2.43) for many different initial phases of mode 1. It will require much computing time. When (2.43a) is used with a proper value of ω, the phase of mode 1 is rotating with angular velocity ω; it is possible to use the time average over a finite period to replace the ensemble average and save much time.

The stationarity of the turbulence is another reason

why we can use the time average to replace the ensemble average. The energy source at mode 1 is continuously supplying the energy to the turbulence to prevent it from decaying. After the early transient process ended, the solutions of (2.43) can be considered a stationary stochastic process, the time average is equal to the ensemble average. In our numerical experiments the time average is taken over the interval from t=10 to t=60 or 110. The numerical results show that the initial conditions have little influence on the outcomes of the time-averaging of the solutions of (2.43), thereby confirm the legality of using the time average.

The energy spectrum E(k), the energy transfer spectrum function R(k) and the energy transfer function Q(k) are given by (2.16)-(2.19), but the r(k) in (2.17) has to be replaced by $r_m(k)$ of (2.36), and the ensemble average is replaced by the time average in the numerical experiments.

2.9. Numerical experiments of Eq. (2.43)

The Adams method is used to solve the initial-value problem of (2.43) up to t=60 Or 110, then the time average from t=10 to t=60 or 110 is used to calculate the energy spectrum E(k) and the energy dissipation rate ϵ. The cut-off wavenumber $k_c = 50$ or 80. The time step $\Delta t=0.005$ for $k_c=0.005$ and $\Delta t=0.0033$ for $k_c=80$, in order for the numerical process to be stable.

The random variable A(k) in (2.41) is constructed by the following procedure. First of all (2.42) is used to produce 5000 random number f(j) uniformly distributed over the interval $(-a,a)$,

$$-a \leqslant f(j) \leqslant a \quad (j=1,2,\ldots,5000) \quad . \tag{2.44}$$

Then for time $t=n\Delta T$ (n=0,1,2,...) the computer generates (k_c-1) pseudo-random integer numbers s(k,n) $(k=2,3,\ldots,k_c)$ which can be any integer between 1 and 5000, by means of (2.42). The ΔT will be defined later. Finally let

$$A(k) = f(s(k,n)) \quad \text{for} \quad n\Delta T \leqslant t \leqslant (n+1)\Delta T \quad . \tag{2.45}$$

The average amplitude of A(k) is $a/2$. The ΔT can be roughly considered the correlation time of the random processes A(k) . In order for P(k) in (2.41) to simulate the pressure term of the Navier-Stokes turbulence as a high-frequency random force, we must let

$$\Delta T \ll 1 \quad . \tag{2.46}$$

In order for the Adams method to be suitable for solving (2.43) which has a rapidly fluctuating term P(k), we must let

$$\Delta T >> \Delta t \quad . \tag{2.47}$$

In the numerical experiments we choose $\Delta T = 10\Delta t$. For example, for $k_c = 50$, $\Delta t = 0.005$, so $\Delta T = 0.05$ which satisfies both (2.46) and (2.47).

More than ten runs of numerical experiments of (2.43) have been made on computer, corresponding to different initial conditions, different cutoff wavenumbers, different sets of random numbers for A(k), different sources and different sinks. We succeed in obtaining the Kolmogorov's $k^{-5/3}$ law for the inertial-range spectrum:

$$E(k) = Ko\, \epsilon^{2/3}\, k^{-5/3} \quad . \tag{2.48}$$

The dimensionless constant Ko is still called the (one-dimensional) Kolmogorov constant. The numerical results of four of these runs are illustrated in Fig. 5-8. The relevant parameters for these numerical experiments are given in Table 3.

The initial conditions and the structure of the energy sink have little influence on the inertial-range spectrum. The influence of the energy sink is limited to the neighborhood of the dissipation range. When the cutoff wavenumber increases from 50 to 80, the inertial-range $3 < k < k_c/4$ becomes wider proportionally, and the Kolmogorov constant seems to

decrease slightly. See Fig. 5-7 and Table 3.

The average amplitude $a/2$ of A(k) has great influence on the spectrum. When a is very small, the term P(k) in (2.31) can be neglected and (2.31) becomes a modified Burgers equation, we get k^{-2} inertial-range spectrum. When a is very large, the term P(k) will be dominant and the advection term can be omitted, the inertial-range spectrum is neither k^{-2} nor $k^{-5/3}$-type. When $1 \leq a \leq 3$, i.e., the average amplitude is between 0.5 and 1.5, both the modified advection term and the pressure-type term are important in (2.31) or (2.43), similar to the case of Navier-Stokes equation, and we obtain the Kolmogorov's $k^{-5/3}$ inertial-range spectrum (2.48). The Kolmogorov constant increases by 10-20 percent as the average amplitude of A(k) increases from 0.5 to 1.5. When using different sets of A(k), we still get the Kolmogorov inertial-range spectrum (2.48) with a slightly different Kolmogorov constant, so long as the average amplitude of A(k) is the same and between 0.5 and 1.5. Figs. 5 to 8 correspond to $a=2$ (so the average amplitude of A(k) is 1).

The introduction of the angular velocity ω in (2.43a) enables us to use the time average over a finite period to replace the ensemble average to calculate the spectrum E(k) and the energy dissipation rate ϵ, but the value of ω can not be too large. When ω is greater than 3 in the case of the modal intensity $\bar{e}(k)=1$, the inertial-range spectrum begins to be different from the Kolmogorov-type (2.48). When

ω increases from 1 to $\pi/2$, the Kolmogorov constant increases a little, see Table 3 and Fig. 6 and 7.

As mentioned in the preceding section, when $\omega=0$ the energy flow rate from mode 1 to higher modes strongly depends on the phase of mode 1. If the phase of mode 1 is $\pi/4$, the energy flow rate is maximum; if the phase of mode 1 is 0, the energy flow rate is nearly zero; if the phase of mode 1 is $\pi/6$, the energy flow rate is medial. Hence we expect that when $\omega=0$ and the phase of mode 1 is $\pi/6$, the time average over a finite period will also correspond to the ensemble average. In order to test this expectation, we use the following initial condition

$$\begin{cases} U(1) = \exp(i\pi/6) & (2.49a) \\ U(k) = 0.31623 \quad \text{if } 2 \leqslant k \leqslant 5 & (2.49b) \\ U(k) = 0.001 \quad \text{if } 6 \leqslant k \leqslant k_c & (2.49c) \end{cases}$$

and let $\omega=0$ in (2.43a), then do the numerical experiment of (2.43). The result is shown in Fig. 8, which confirms the above expectation.

The (one-dimensional) Kolmogorov constant obtained in our numerical experiments of (2.43) ranges from 0.5 to 0.65. Ko=0.5 is obtained in the case of $\omega=1$, $k_c=80$ and $a=1$. Ko=0.65 is obtained in the case of $\omega=\pi/2$, $k_c=50$ and $a=3$.

The outcomes of the time-averaging over longer time interval are more smooth and have less fluctuation. Fig. 7 is for interval from t=10 to t=110; Fig. 5,6 and 8 are for t=10 to t=60.

CHAPTER III. VARIATIONAL APPROACH APPLIED TO ONE-DIMENSIONAL TURBULENCE

According to the numerical experiments, the one-dimensional model of turbulence (2.31) has the Kolmogorov's $k^{-5/3}$ inertial-range spectrum and the corresponding (one-dimensional) Kolmogorov constant ranges from 0.5 to 0.65. It gives us an opportunity to test further the validity and error of the variational approach to the closure problem of turbulence proposed in Chapter I.

First of all we introduce a complete set of independent real modal parameters for the one-dimensional turbulence (2.31), and transform the dynamic equation (2.31) into a form similar to the form of Eq. (1.5) in terms of this complete set of real parameters. Then most of the results of Sections 1.2-1.8 can be applied to the one-dimensional turbulence without much change. Finally the Kolmogorov's $k^{-5/3}$ law is derived and the (one-dimensional) Kolmogorov constant is numerically evaluated, giving Ko=0.55 which is in good agreement with the results of the numerical experiments of (2.43).

In order to use the results of Chapter I as much as possible, we will use the same notation as in Chapter I. The readers are advised to keep in mind that in this Chapter we deal with an one-dimensional turbulence.

3.1. Complete set of independent real parameters

The complex modal parameters $U(k)=U^{(1)}(k)+iU^{(2)}(k)$ satisfy the 'realness' condition $U(-k)=U^*(k)$, i.e.,

$$U^{(1)}(-k) = U^{(1)}(k) \text{ and } U^{(2)}(-k) = -U^{(2)}(k) \quad . \tag{3.1}$$

Hence the complex modal parameters are not independent. As done for the three-dimensional case, the wavenumber k and the real-imaginary-part index α are combined into one index i, i.e., let

$$i = (\alpha, k) \quad , \quad -i = (\alpha, -k) \quad , \tag{3.2}$$

and $i>0$ if $k>0$. The real modal parameters is

$$X_i = S(i)U^{(\alpha)}(k) \quad , \tag{3.3}$$

here S(i) is defined by (A.17) in Appendix A. Then Eq. (3.1) means that

$$X_i = X_{-i} \quad . \tag{3.4}$$

Hence $(X_i, i\geq 0)$ forms a complete set of independent real modal parameters for the one-dimensional turbulence.

Similar to the derivation given in Appendix A, from (2.31) and (3.1)-(3.4), we have

$$(\frac{d}{dt} + \nu_i)X_i = \sum_{j,m} A_{ijm}X_jX_m + F_i^{(p)} \quad . \tag{3.5}$$

Here $\nu_i=\nu(k)$; and

$$A_{ijm} = 0 \quad \text{if any two of } i,j,m \text{ are equal} \quad , \tag{3.6}$$

otherwise

$$A_{ijm} = (\tfrac{k}{2})S(i)C^{\alpha\beta\gamma}\left[S(j)S(m)\delta_{k,p+r} + S(j)S(-m)\delta_{k,p-r}\right.$$
$$\left. + S(-j)S(m)\delta_{k,-p+r} + S(-j)S(-m)\delta_{k,-p-r}\right] \quad , \tag{3.7}$$

here $C^{\alpha\beta\gamma}$ is defined by Table 1. The $F_i^{(p)}$ in (3.5) corresponds to the pressure-type term P(k) in (2.31) and (2.41), and

$$F_i^{(p)} = -\begin{cases} -S(i)U^{(2)}(k)A(k)|U(1)|^2/|U(k)| & \text{if } \alpha=1 \\ \\ S(i)U^{(1)}(k)A(k)|U(1)|^2/|U(k)| & \text{if } \alpha=2 \end{cases} \quad . \tag{3.8}$$

If the source term $\mathcal{M}(k)U(k)$ is introduced into (2.31), (3.5) becomes

$$\frac{d}{dt}X_i = -(\nu_i-\nu_i')X_i + \sum_{j,m}A_{ijm}X_jX_m + F_i^{(p)} \quad . \tag{3.9}$$

Here $\nu_i'=\mathcal{M}(k)$ which is zero at high wavenumbers.

3.2. Liouville equation and perturbàtion solution

Similar to the three-dimensional case, by classical mechanics all possible dynamic states of the one-dimensional turbulence, or all possible $(X_i, i\geq 0)$, constitute a phase space. The Liouville equation for the probability distribution P in the phase space is

$$\frac{\partial P}{\partial t} + (\bar{L} + \bar{L}^{(p)})P = 0 \quad , \tag{3.10}$$

where

$$\bar{L} = -\sum_i \left((\nu_i - \nu_i')\frac{\partial}{\partial X_i}X_i - \sum_{j,m} A_{ijm}X_jX_m\frac{\partial}{\partial X_i} \right) \quad , \tag{3.11}$$

$$\bar{L}^{(p)} = \sum_i \frac{\partial}{\partial X_i} F_i^{(p)} \quad . \tag{3.12}$$

According to a Langevin-Fokker-Planck model similar to that in Chapter I, we have

$$\sum_{j,m} A_{ijm}X_jX_m + F_i^{(p)} \simeq -\zeta_i X_i + f_i \tag{3.13}$$

and

$$\bar{L} + \bar{L}^{(p)} \simeq \bar{L}^{(f)} \quad , \tag{3.14}$$

here

$$\bar{L} = -\sum_i \eta_i \left(\frac{\partial}{\partial X_i}X_i + \phi_i \frac{\partial^2}{\partial X_i^2} \right) \tag{3.15}$$

is the Fokker-Planck operator, corresponding to the Langevin equation

$$\frac{d}{dt}X_i = -\eta_i X_i + f_i \quad , \quad \eta_i = \zeta_i + \nu_i - \nu_i' \quad . \tag{3.16}$$

The f_i in (2.13) and (2.16) is a random force of the type of white noise. For the inertial-range, $\nu_i = \nu_i' = 0$, we have

$$\eta_i = \zeta_i \tag{3.17}$$

For a stationary one-dimensional turbulence, the Liouville equation can be written as follows

$$\left(\bar{L}^{(f)} + \left(\bar{L} + \bar{L}^{(p)} - \bar{L}^{(f)} \right) \right) P = 0 \quad . \tag{3.18}$$

According to (3.13) (3.14), $(\bar{L}+\bar{L}^{(p)}-\bar{L}^{(f)})$ is to be considered a small perturbation operator. Hence the approximate solution of (3.18) at zero order, denoted by $P^{(0)}$, satisfies

$$\bar{L}^{(f)} P^{(0)} = 0 \quad . \tag{3.19}$$

Eq. (3.19) is Fokker-Planck equation, its solution is the Gaussian function (1.18). Let

$$P = P^{(0)} + P^{(1)} \quad , \tag{3.20}$$

similar to (1.20) we have

$$\bar{L}^{(f)} P^{(1)} = -(\bar{L}+\bar{L}^{(p)}-\bar{L}^{(f)}) P^{(0)} = -(\bar{L}+\bar{L}^{(p)}) P^{(0)} . \tag{3.21}$$

In Appendix C we have proved that $\bar{L}^{(p)} P^{(0)} = 0$, so (3.21) becomes

$$\bar{L}^{(f)} P^{(1)} = -\bar{L} P^{(0)} \quad . \tag{3.22}$$

Similar to the derivation from (1.20) to (1.23), we have

$$P = \left[1 - \sum_i (\nu_i - \nu_i') \frac{X_i^2 - \phi_i}{2 \eta_i \phi_i} + \sum_{ijm} \frac{A_{ijm} X_i X_j X_m}{\phi_i (\eta_i + \eta_j + \eta_m)} \right] P^{(0)} \quad . \tag{3.23}$$

3.3. Energy equation

Using the Liouville equation (3.10)-(3.12), we have

$$\frac{d}{dt}\langle X_i^2\rangle = \int X_i^2 (\frac{\partial P}{\partial t}) \prod dX_n = -\int X_i^2 (\bar{L}+\bar{L}^{(p)}) P \prod dX_n =$$

$$= -2(\nu_i - \nu_i')\langle X_i^2\rangle + 2\sum_{j,m} A_{ijm}\langle X_i X_j X_m\rangle - \int X_i^2 \bar{L}^{(p)} P \prod dX_n \ . \tag{3.24}$$

From (2.9) (2.16) (3.1) and (3.3), we have

$$E(k) = \sum_{\alpha=1}^{2}\langle X_i^2\rangle = 2\langle X_i^2\rangle \tag{3.25}$$

Substitute (3.25) into (3.24), we have (neglecting ν_i')

$$(\frac{d}{dt} + 2\nu(k))E(k) = 4\sum_{j,m} A_{ijm}\langle X_i X_j X_m\rangle - \int \left(\sum_{\alpha=1}^{2} X_i^2\right) \bar{L}^{(p)} P \prod dX_n \ . \tag{3.26}$$

In Appendix C we have proved that the last term of (3.26) is zero, so

$$(\frac{d}{dt} + 2\nu(k))E(k) = 4\sum A_{ijm}\langle X_i X_j X_m\rangle \ . \tag{3.27}$$

Using probability distribution (3.23), (3.27) becomes

$$(\frac{d}{dt} + 2\nu(k))E(k) = T(k) \ , \tag{3.28}$$

$$T(k) = 2\sum_{j,m} \frac{A_{ijm}\left(A_{ijm}E(p)E(r)+A_{jmi}E(k)E(r)+A_{mij}E(k)E(p)\right)}{\eta_i + \eta_j + \eta_m} \ . \tag{3.29}$$

Using an integral to approximate the summation, by (3.6) and (3.7) we can prove the following formula for a continuous

function f(k,p,r) of k,p,r:

$$\sum_{j,m}' f(k,p,r)A_{ijm}A_{ijm} \simeq \frac{k^2}{2}\int_{-\infty}^{+\infty} f(k,p,k-p)dp \quad , \tag{3.30a}$$

$$\sum_{j,m}' f(k,p,r)A_{ijm}A_{jmi} \simeq -\frac{k}{2}\int_{-\infty}^{+\infty} f(k,p,k-p)pdp \quad , \tag{3.30b}$$

$$\sum_{j,m}' f(k,p,r)A_{ijm}A_{mij} \simeq -\frac{k}{2}\int_{-\infty}^{+\infty} f(k,p,k-p)(k-p)dp \quad . \tag{3.30c}$$

Substitute (3.30) into (3.29), we have

$$T(k) = \int_{-\infty}^{+\infty} \frac{k^2E(p)E(r) - kpE(k)E(r) - krE(k)E(p)}{\eta(k) + \eta(p) + \eta(r)}\, dp \quad , \tag{3.31}$$

with k=p+r.

3.4. Energy transfer function

The energy transfer spectrum function T(k) given by (3.31) can be written as

$$T(k) = \int_{-\infty}^{+\infty} dp \int_{-\infty}^{+\infty} dr\ S^*(p,r;k) \ , \tag{3.32}$$

$$S^*(p,r;k) = k\delta(k-p-r)\frac{kE(p)E(r)-pE(k)E(r)-rE(k)E(p)}{\eta(k)+\eta(p)+\eta(r)} \ . \tag{3.33}$$

In order to see the physical meaning of (3.32) more clearly, it is convenient to work with positive values only. So we rewrite (3.32) as follows

$$T(k) = \int_0^{\infty} dp \int_0^{\infty} dr \ \Big(S^*(p,r;k)+S^*(-p,r;k)+S^*(p,-r;k) + S^*(-p,-r;k) \Big) \ . \tag{3.34}$$

For positive k,p,r, $S^*(-p,-r;k)=0$, so we have

$$T(k) = \int_0^{\infty} dp \int_0^{\infty} dr\ \bar{S}(p,r;k) \ , \tag{3.35}$$

$$\bar{S}(p,r;k) = S^*(p,r;k)+S^*(-p,r;k)+S^*(p,-r;k) \ . \tag{3.36}$$

Their physical meaning is that $\bar{S}(p,r;k)dkdpdr$ gives the rate of energy transfer into modes (k,k+dk) due to the nonlinear interaction between modes (p,p+dp) and (r,r+dr) with the constraint k=p+r. It can be proved that

$$\bar{S}(p,r;k) + \bar{S}(r,k;p) + \bar{S}(k,p;r) = 0 \ , \tag{3.37}$$

which expresses the detailed conservation of energy for the

microdynamic processes.

The energy transfer function is

$$\Pi(k) = \int_k^\infty dk' T(k') \quad . \tag{3.38}$$

From (3.35) (3.36) (3.38), after long manipulation, we have

$$\Pi(k) = 2\int_{-k}^{k} dp \int_{p^*}^{\infty} dr\, \tilde{k}\, \frac{\tilde{k}E(p)E(r) - pE(\tilde{k})E(r) - rE(\tilde{k})E(p)}{\eta(\tilde{k}) + \eta(p) + \eta(r)} \quad , \tag{3.39}$$

with $\tilde{k}=p+r$. Here

$$p^* = \max(p,\ k-p) \quad . \tag{3.40}$$

In the inertial-range the energy transfer function $\Pi(k)$ is independent of k, and is equal to the energy dissipation rate $\epsilon = 2\int_0^\infty \nu(k)E(k)dk$, therefore

$$\epsilon = 2\int_{-k}^{k} dp \int_{p^*}^{\infty} dr\, \tilde{k}\, \frac{\tilde{k}E(p)E(r) - pE(\tilde{k})E(r) - rE(\tilde{k})E(p)}{\eta(\tilde{k}) + \eta(p) + \eta(r)} \quad , \tag{3.41}$$

with $\tilde{k}=p+r$.

3.5. The η equation

The validity and error of the perturbation solution (2.31) depends on the 'smallness' of the operator $(\bar{L}+\bar{L}^{(p)}-\bar{L}^{(f)})$, and thus on the validity and error of the approximation (3.13). We treat ζ_i or η_i in (3.13)-(3.16) as optimum control parameters to minimize the error of the approximation (3.13). The 'optimum' is interpreted in the mean-square sense, i.e., we choose ζ_i or η_i in such a way that

$$\sum_i \left\langle \left(\sum_{j,m} A_{ijm} X_j X_m + F_i^{(p)} - (-\zeta_i X_i) \right)^2 \right\rangle \tag{3.42}$$

is minimum. According to the structure of $F_i^{(p)}$ given by (3.8), there is no correlation between $F_i^{(p)}$ and X_i due to the randomness of A(k). Moreover $\langle (F_i^{(p)})^2 \rangle$ is independent of ζ_i. Hence the minimization of (3.42) leads to

$$\eta_i = 4 \sum_{j,m} \frac{B_{ijm}(\eta_j A_{jim} + \eta_m A_{mij} - (\eta_j + \eta_m) A_{ijm})}{E(k)(\eta_i + \eta_j + \eta_m)^2} , \tag{3.43}$$

$$B_{ijm} = \frac{1}{4}(A_{ijm}E(p)E(r) + A_{jmi}E(k)E(r) + A_{mij}E(k)E(p)) . \tag{3.44}$$

Similar to (3.30), we can prove that

$$\sum_{j,m} f(k,p,r) A_{jim} A_{jim} \simeq \frac{1}{2} \int_{-\infty}^{+\infty} f(k,p,k-p) p^2 dp , \tag{3.45a}$$

$$\sum_{j,m} f(k,p,r) A_{jim} A_{mij} \simeq \frac{1}{2} \int_{-\infty}^{+\infty} f(k,p,k-p) p(k-p) dp . \tag{3.45b}$$

By uing (3.30) and (3.45), similar to the derivation from (3.29) to (3.31), (3.43) becomes

$$\eta(k)E(k) = \int_{-\infty}^{+\infty} \hat{dp} \frac{\eta(p)}{(\eta(k)+\eta(p)+\eta(r))^2} \Big[kpE(r)(E(k)-E(p)) + k^2E(p)(E(k)-E(r)) + p^2E(k)(E(r)-E(p))\Big] \quad , \tag{3.46}$$

with $k=p+r$.

Eqs. (3.41) (or (3.28) with (3.31)) and (3.46) form a closed set of integral equations for two unknown functions $E(k)$ and $\eta(k)$. As an application of this closed set of integral equations, in next section we will derive the Kolmogorov's $k^{-5/3}$ inertial-range spectrum (2.48), and calculate the corresponding Kolmogorov constant theoretically.

3.6. Kolmogorov law and Kolmogorov constant

Following the same procedure of Section 1.9, we suppose that in the inertial-range $E(k)$ and $\eta(k)$ have the form of power functions

$$E(k) = Ak^m \quad \text{and} \quad \eta(k) = Bk^n \quad . \tag{3.47}$$

Substitute (3.47) into (3.41) and (3.46), and we obtain

$$4 + 2m - n = 0 \quad \text{and} \quad 3 + m - 2n = 0 \quad . \tag{3.48}$$

Hence $m=-5/3$ and $n=2/3$. Let $A=Ko\epsilon^{2/3}$ and $B=D\epsilon^{1/3}$, so that (3.47) becomes

$$E(k) = Ko\epsilon^{2/3}k^{-5/3} \quad , \tag{3.49}$$

$$\eta(k) = D\epsilon^{1/3}K^{2/3} \quad . \tag{3.50}$$

Eq. (3.49) is the Kolmogorov's inertial-range law.

Substituting (3.49) and (3.50) into (3.41) and (3.46), and then calculating the two resulting integrals by numerical method, we have

$$D/Ko^2 = 2.05 \quad , \quad D^2/Ko = 0.68 \quad . \tag{3.51}$$

From (3.51) the Kolmogorov constant is

$$Ko = 0.55 \quad , \tag{3.52}$$

which is in good agreement with the results of the numerical experiments reported in Chapter II (which gives that Ko ranges from 0.5 to 0.65). The success of the variational approach to the closure problem is encouraging.

CONCLUDING REMARKS

We proposed a new (variational) approach to solve the closure problem of turbulence theory in an Eulerian framework. By this approach, starting from the first principle of the statistical mechanics, we derived the Kolmogorov $k^{-5/3}$ inertial-range spectrum and evaluate the Kolmogorov constant.

The Kraichnan's DI approximation deals with multi-time correlations. Its Eulerian formulation meets divergence difficulty and is unsuitable for deriving Kolmogorov law. The variational approach proposed in this thesis deals with single-time correlations only, so it can solve the closure problem in an Eulerian framework and implies the Kolmogorov law.

The Edwards and McComb's entropy method is also an Eulerian closure approximation and implies the Kolmogorov law, but gives a poor value of Kolmogorov constant. Its underlying physical idea is questionable because they apply the principle of maximum entropy (which is valid for an isolated system at thermodynamic equilibrium) to a system that is far away from thermodynamic equilibrium and interacts with its surroundings.

Actually we need not appeal to another physical principle. The correct way to find another proper equation for q and η should be intrinsically related to the LFP model itself as well as the essence of the η. That is the method we

have used in this thesis.

At present we have no formal proof of the convergence of the perturbation method introduced in Section 1.4. A relevant problem is the possibility of the perturbation solution (1.23) being negative when the modal parameter X_i is very large. It is similar to the situation in the Chapman-Enskog nonequilibrium theory of dilute gases, where the probability distribution of molecular velocity (obtained as the perturbation solution of the Boltzmann's equation) has a form similar to (1.23) and also becomes negative when the molecular velocity is very large[39,40]. We know that the Chapmann-Enskog nonequilibrium theory is a quite satisfactory one for the transport phenomena of dilute gases and is confirmed by experiments. In our opinion, there are two reasons why we can use the perturbation solution (1.23) as an approximation of the exact probability distribution despite its possible negativeness. First, the probability of X_i being large is small. Second, the two perturbation terms in (1.23) are the summations over all modes, and the number of modes is infinite; due to the law of large number of probability theory, the probability of the two perturbation terms being large enough becomes much smaller. Therefore, although we cannot exclude the 'events' which make the perturbation solution (1.23) negative, the measure of the set of these 'events' in probability space is very small or nearly zero, therefore their contribution to the statistical properties of turbulence can be neglected.

The argument, which leads Kolmogorov to propose the $k^{-5/3}$ law for the inertial-range spectrum of turbulence[41], is so general that it is logical to expect that the Kolmogorov's $k^{-5/3}$ law is valid despite the dimensionality of turbulence. Unfortunately the commonly-used one-dimensional model of turbulence (the Burgers turbulence) has k^{-2} inertial-range spectrum instead of $k^{-5/3}$. Hence two questions arise. The first one is: what is the essential difference between the Burgers equation and the Navier-Stokes equation which leads to the different inertial-range spectrums. The second question (which is more challenging) is: how to find a proper one-dimensional model of turbulence which has the Kolmogorov's $k^{-5/3}$ inertial-range spectrum. We hope the research reported in Chapter II can help to answer the two questions.

The numerical experiments reported in this thesis confirm the vital role of the pressure term in hydrodynamic turbulence. The advection term builds up the correlation between modes and reduces the chaos of the flow field, and finally all modes are precisely locked in phase over the entire spectrum. The nonlinear interaction of advection alone can not generate turbulence. The pressure term acts as a high-frequency conservative random force to limit the build-up of correlation between modes and to destroy the spectrum-wide phase locking, finally leading to a turbulence with Kolmogorov's $k^{-5/3}$ spectrum for the inertial-range.

In the author's opinion the difference between Burgers equation and the Navier-Stokes equation is more interesting than their similarity. It is significant to have a one-dimensional model of the Navier-Stokes equation, which yields Kolmogorov's $k^{-5/3}$ inertial-range spectrum. In this thesis we are successful in proposing such a one-dimensional model. Of course it is not the unique and best one-dimensional model of turbulence which has a Kolmogorov-type inertial-range spectrum. The numerical experiments on this one-dimensional turbulence provide an opportunity to test various approaches to the closure problem of turbulence theory. We used them to test the variational approach proposed in this thesis and showed that the success of the variational approach is encouraging, as mentioned in Chapter III.

It is advised to consider the one-dimensional model (2.31) or (2.43) a purely mathematical model of hydrodynamic turbulence. It is not recommended to transform the one-dimensional model (2.31) into (t,x) space and to extract the 'physical meaning' of the resulting equation. The most important thing is that the model (2.31) can similate the essential feature of the cascade transfer of energy in a turbulence and has a Kolmogorov's $k^{-5/3}$ inertial-range spectrum.

Our numerical experiments are over a wavenumber range of 50-100. Of course nowadays computers allow us to do numerical studies of the (3-dimensional) Navier-Stokes equation over a wavenumber range of almost the same order and a

numerical study of the Burgers equation over a wavenumber range of thousands. But the numerical study of the Navier-Stokes equation over a wavenumber range of the same order (e.g. 32) could hardly provide any significant information on the inertial-range dynamics of a turbulence. For our numerical experiments the wavenumber range of 50-100 is wide enough to produce an inertial range containing enough experimental data to indicate whether the spectrum is k^{-2} or $k^{-5/3}$ and in the case of $k^{-5/3}$ to obtain a quite accurate Kolmogorov constant.

APPENDIX A. MODAL PARAMETERS AND MODAL DYNAMIC EQUATIONS

The Fourier components $u_i(\underline{k})$ are not independent, because of (1.4). In order to define independent modal parameters, we introduce two orthogonal unit vector, $\underline{n}_1(\underline{k})$ and $\underline{n}_2(\underline{k})$, in the plane perpendicular to the wavevector $\underline{k}$, so that $\underline{n}_1(\underline{k})$, $\underline{n}_2(\underline{k})$ and $\underline{n}_3(\underline{k})=(\text{sign}(k_3)/k)/\underline{k}$ form a right-handed orthonormal triad. The factor $\text{sign}(k_3)$ makes $\underline{n}_3(\underline{k})$ always point upwards. Let

$$\underline{n}_a(\underline{k})= (n_{a1}(\underline{k}), n_{a2}(\underline{k}), n_{a3}(\underline{k})) \quad , \tag{A.1}$$

so $n_{ai}(\underline{k})$ is the ith component of vector $\underline{n}_a(\underline{k})$, it is easy to prove the following formula for $n_{ai}(\underline{k})$,

$$n_{ai}(-\underline{k}) = n_{ai}(\underline{k}) \quad , \tag{A.2}$$

$$n_{3i}(\underline{k})u_i(\underline{k}) = 0 \quad , \tag{A.3}$$

$$n_{3i}(\underline{k})P_{ij}(\underline{k}) = n_{3j}(\underline{k})P_{ij}(\underline{k}) = 0 \quad , \tag{A.4}$$

(afterwards the indexes a,b,c are restricted to take value 1 or 2 only)

$$n_{ai}(\underline{k})P_{ij}(\underline{k}) = n_{aj}(\underline{k}) \quad , \tag{A.5}$$

$$n_{ai}(\underline{k})n_{aj}(\underline{k}) = P_{ij}(\underline{k}) \quad . \tag{A.6}$$

Let

$$V_a(\underline{k}) = n_{ai}(\underline{k})u_i(\underline{k}) \quad , \tag{A.7}$$

therefore

$$u_i(\underline{k}) = V_a(\underline{k}) n_{ai}(\underline{k}) \quad . \tag{A.8}$$

Using (A.5) (A.7) and (A.8), the Navier-stokes equation (1.1) becomes

$$(\frac{d}{dt}+\nu k^2)V_a(\underline{k}) = -iH\sum_{\underline{p},\underline{r}} P_{abc}(\underline{k},\underline{p},\underline{r})\delta_{\underline{k},\underline{p}+\underline{r}} V_b(\underline{p})V_c(\underline{r}) \quad , \tag{A.9}$$

where

$$P_{abc}(\underline{k},\underline{p},\underline{r}) = \tfrac{1}{2}(k_m n_{aj}(\underline{k})+k_j n_{am}(\underline{k}))n_{bj}(\underline{p})n_{cm}(\underline{r}) \quad . \tag{A.10}$$

From (1.4) (A.2) and (A.7), we have

$$V_a(\underline{k}) = V_a^*(-\underline{k}) \quad . \tag{A.11}$$

Hence $V_a(\underline{k})$ are not independent. Let $V_a^{(1)}(\underline{k})$ and $V_a^{(2)}(\underline{k})$ be the real and imaginary part of $V_a(\underline{k})$ respectively, then (A.11) means that

$$V_a^{(1)}(\underline{k}) = V_a^{(1)}(-\underline{k}) \quad , \quad V_a^{(2)}(\underline{k}) = -V_a^{(2)}(-\underline{k}) \quad . \tag{A.12}$$

Introducing $V_a(\underline{k})=V_a^{(1)}+iV_a^{(2)}$ into (A.9), we have

$$(\frac{d}{dt}+\nu k^2)V_a^{(\alpha)}(\underline{k}) = H\sum_{\underline{p},\underline{r}} P_{abc}(\underline{k},\underline{p},\underline{r})C^{\alpha\beta\gamma}\delta_{\underline{k},\underline{p}+\underline{r}} V_b^{(\beta)}(p)V_c^{(\gamma)}(\underline{r}) \quad , \tag{A.13}$$

where the $C^{\alpha\beta\gamma}$ is defined by the Table 1.

The discrete countable wavevector '$\underline{k}$', component index 'a' and real-imaginary-part index 'α' are lumped together to form a single index 'i' in the following way

$$i = (\alpha, a, \underline{k}) , \quad -i = (\alpha, a, -\underline{k}) , \tag{A.14}$$

$$i>0 \quad \text{if } (k_3>0) \text{ or } (k_2>0, k_3=0) \text{ or } (k_1>0, k_2=k_3=0) . \tag{A.15}$$

The new modal parameters X_i are defined as follows

$$X_i = S(i)V_a^{(\alpha)}(\underline{k}) , \tag{A.16}$$

where

$$S(i) = -1 \quad \text{if } (i<0, \alpha=2), \quad \text{otherwise } S(i) = 1, \tag{A.17}$$

thereby we have $S(i)S(i)=1$. By using (A.14)-(A.17), Eq. (A.13) becomes

$$(\frac{d}{dt}+\nu_i)X_i = \sum_{j,m} M_{ijm}X_jX_m , \tag{A.18}$$

where $\nu_i=\nu k^2$, and

$$M_{ijm} = HS(i)S(j)S(m)P_{abc}(\underline{k},\underline{p},\underline{r})C^{\alpha\beta\gamma}\delta_{\underline{k},\underline{p}+\underline{r}} . \tag{A.19}$$

According to (A.14)-(A.17), Eq.(A.12) is equivalent to

$$X_{-i} = X_i , \tag{A.20}$$

therefore (X_i, $i\geq 0$) forms a complete set of independent real modal parameters of turbulence. From (A.18), the dynamic equation for the independent real modal parameters are

$$(\frac{d}{dt}+\nu_i)X_i = \sum_{j=0}^{\infty}\sum_{m=0}^{\infty} A_{ijm}X_jX_m = \sum_{j,m} A_{ijm}X_jX_m , \tag{A.21}$$

where

$$A_{ijm} = M_{ijm}+M_{ij-m}+M_{i-jm}+M_{i-j-m} . \tag{A.22}$$

Some useful properties of M_{ijm} are

$$M_{ijm} = M_{imj} \quad , \tag{A.23}$$

$$M_{-i-j-m} = M_{ijm} \quad , \tag{A.24}$$

$$M_{ijm} = 0 \quad \text{if any two of i,j,m are equal} \quad . \tag{A.25}$$

From (A.19) (A.22) and (A.23)-(A.25), we can prove that

$$A_{ijm} = A_{imj} \quad , \tag{A.26}$$

$$A_{ijm} = 0 \quad \text{if any two of i,j,m are equal} \quad . \tag{A.27}$$

Do not confuse the indexes i,j,m in (A.14)-(A.27) with those in (2.1)-(2.4) and (A.1)-(A.13).

APPENDIX B. IMPORTANT FORMULA FOR A_{ijm}

All the formula, needed for the derivations in Sections 1.7 and 1.8, are given below. Their detailed derivations are too long to be listed here. Suppose f(k,p,r) is any function of k,p,r, by using the formula in Appendix A and the Table 1, we can prove the following formula

$$\sum_{j,m} f(k,p,r)A_{ijm}A_{jim} = -\bar{C}\sum_{\underline{p},\underline{r}} f(k,p,r)J_3(k,p,r)\delta_{\underline{k},\underline{p}+\underline{r}} \quad , \quad (B.1)$$

$$\sum_{j,m} f(k,p,r)A_{ijm}A_{mij} = -\bar{C}\sum_{\underline{p},\underline{r}} f(k,p,r)J_3(k,r,p)\delta_{\underline{k},\underline{p}+\underline{r}} \quad , \quad (B.2)$$

$$\sum_{j,m} f(k,p,r)A_{ijm}A_{ijm} = +\bar{C}\sum_{\underline{p},\underline{r}} f(k,p,r)J_1(k,p,r)\delta_{\underline{k},\underline{p}+\underline{r}} \quad , \quad (B.3)$$

$$\sum_{j,m} f(k,p,r)A_{jim}A_{mij} = -\bar{C}\sum_{\underline{p},\underline{r}} f(k,p,r)J_3(p,r,k)\delta_{\underline{k},\underline{p}+\underline{r}} \quad , \quad (B.4)$$

$$\sum_{j,m} f(k,p.r)A_{jim}A_{jim} = +\bar{C}\sum_{\underline{p},\underline{r}} f(k,p,r)J_1(p,k,r)\delta_{\underline{k},\underline{p}+\underline{r}} \quad , \quad (B.5)$$

where $\bar{C}=\frac{1}{4}H^2$ and $H=(2\pi/L)^3$, J_1 and J_3 are the same as used by Kraichnan[1].

$$J_3(k,p,r) = J_3(p,k,r) = 2kp(xy+z^3) \quad , \quad (B.6)$$

$$J_3(p,r,k) = J_3(r,p,k) = 2pr(yz+x^3) \quad , \quad (B.7)$$

$$J_1(k,p,r) = J_3(k,p,r) + J_3(k,r,p) \quad , \quad (B.8)$$

$$J_1(p,k,r) = J_3(p,k,r) + J_3(p,r,k) \quad , \quad (B.9)$$

where

$$x = \frac{p^2+r^2-k^2}{2pr} \quad , \quad y = \frac{r^2+k^2-p^2}{2kr} \quad , \quad z = \frac{p^2+k^2-r^2}{2kp} \qquad \text{(B.10)}$$

are the cosines of three angles of the triangle with sides k, p and r. Kraichnan et al use the geometrical factor b(k,p,r) to express $J_3(k,p,r)$,

$$J_3(k,p,r) = 2k^2 b(k,p,r), \quad b(k,p,r) = \frac{p}{k}(xy+z^3) \quad . \qquad \text{(B.11)}$$

When the cubic box, introduced at the beginning of Section 1.1, becomes infinitely large, i.e., when $L \to \infty$, the summation in (B.1)-(B.5) becomes integrals, and

$$(1/H)\delta_{\underline{k},\underline{p}+\underline{r}} \longrightarrow \delta(\underline{k}-\underline{p}-\underline{r}) \quad , \qquad \text{(B.12)}$$

here $\delta(\underline{k}-\underline{p}-\underline{r})$ is Dirac delta function. The transform of the bipolar integral is

$$\iint f(k,p,r)\delta(\underline{k}-\underline{p}-\underline{r})dpdr = \iint_{\Delta} (2\pi pr/k)f(k,p,r)dpdr \quad , \qquad \text{(B.13)}$$

here Δ indicates that the integration is restricted to the following infinite slot in the first quarter of the p-r plane[1],

$$\Delta : (r \geqslant 0, |k-r| \leqslant p \leqslant |k+r|) \text{ or } (p \geqslant 0, |k-p| \leqslant r \leqslant |k+p|) \quad . \qquad \text{(B.14)}$$

APPENDIX C. PROPERTIES OF $\bar{L}^{(p)}$

The operator $L^{(p)}$ defined by (3.12) corresponds to the force $F_i^{(p)}$ given by (3.8). The force $F_i^{(p)}$ has the following important property

$$\sum_{\alpha=1}^{2} X_i F_i^{(p)} = 0 \ . \tag{C.1}$$

From (2.9) and (3.3), we have

$$\bar{e}(k) = \sum_{\alpha=1}^{2} X_i^2 \ . \tag{C.2}$$

The physical meaning of (C.1) is that any function of the modal intensity $\bar{e}(k)$ is a constant of motion for the force $F_i^{(p)}$. Hence the operator $\bar{L}^{(p)}$ has the following properties

$$\bar{L}^{(p)} F(\bar{e}(k)) = 0 \ , \tag{C.3}$$

$$\int F(\bar{e}(k)) \bar{L}^{(p)} P \prod dX_n = 0 \ . \tag{C.4}$$

where $F(\bar{e}(k))$ is any function of the modal intensity $\bar{e}(k)$ and P is the probability distribution. As special cases of (C.3) and (C.4), we have

$$\bar{L}^{(p)} P^{(0)} = 0 \ , \tag{C.5}$$

$$\int \bar{e}(k) \bar{L}^{(p)} P \prod dX_n = \int \left[\sum_{\alpha=1}^{2} X_i^2 \right] \bar{L}^{(p)} P \prod dX_n = 0 \ . \tag{C.6}$$

Table 1. Definition of $C^{\alpha\beta\gamma}$

α	β	γ	$C^{\alpha\beta\gamma}$
1	1	1	0
1	1	2	1
1	2	1	1
1	2	2	0
2	1	1	-1
2	1	2	0
2	2	1	0
2	2	2	1

Table 2 Parameters for numerical experiments of Eq.(2.26) (Fig. 1-4)

Run No.	Initial condition	Cut-off wavenumber k_c	Energy sink ν_d	Energy sink n	Energy sink k_d	Time step Δt
1	Eq.(2.27)	50	0.2	3	40	0.005
2	Eq.(2.28)	50	0.2	3	40	0.005
3	Eq.(2.29)	50	0.2	3	40	0.005
4	Eq.(2.30)	50	0.2	3	40	0.005
5	Eq.(2.27)	50	0.25	2	30	0.005
6	Eq.(2.29)	50	0.25	2	30	0.005
7	Eq.(2.27)	100	0.2	2	60	0.0025
8	Eq.(2.28)	100	0.2	2	60	0.0025
9	Eq.(2.29)	100	0.2	2	60	0.0025
10	Eq.(2.30)	100	0.2	2	60	0.0025

Table 3. Parameters for numerical experiments of Eq.(2.43) (Fig. 5-8)

Fig. No.	Initial Condition	Cut-off wavenumber k_c	Energy source ω	Energy sink ν_d	n	k_d	Interval of time average	Dissipation rate ϵ	Kolmogorov constant Ko
5	Eq.(2.28)	80	$\pi/2$	0.2	2	50	10-60	0.470	0.60
6	Eq.(2.28)	50	$\pi/2$	0.1	3	40	10-60	0.451	0.63
7	Eq.(2.28)	50	1	0.1	2	30	10-110	0.645	0.58
8	Eq.(2.49)	50	0	0.2	2	30	10-60	0.457	0.61

(The average amplitude of A(k) is /2 for Fig. 5-8)

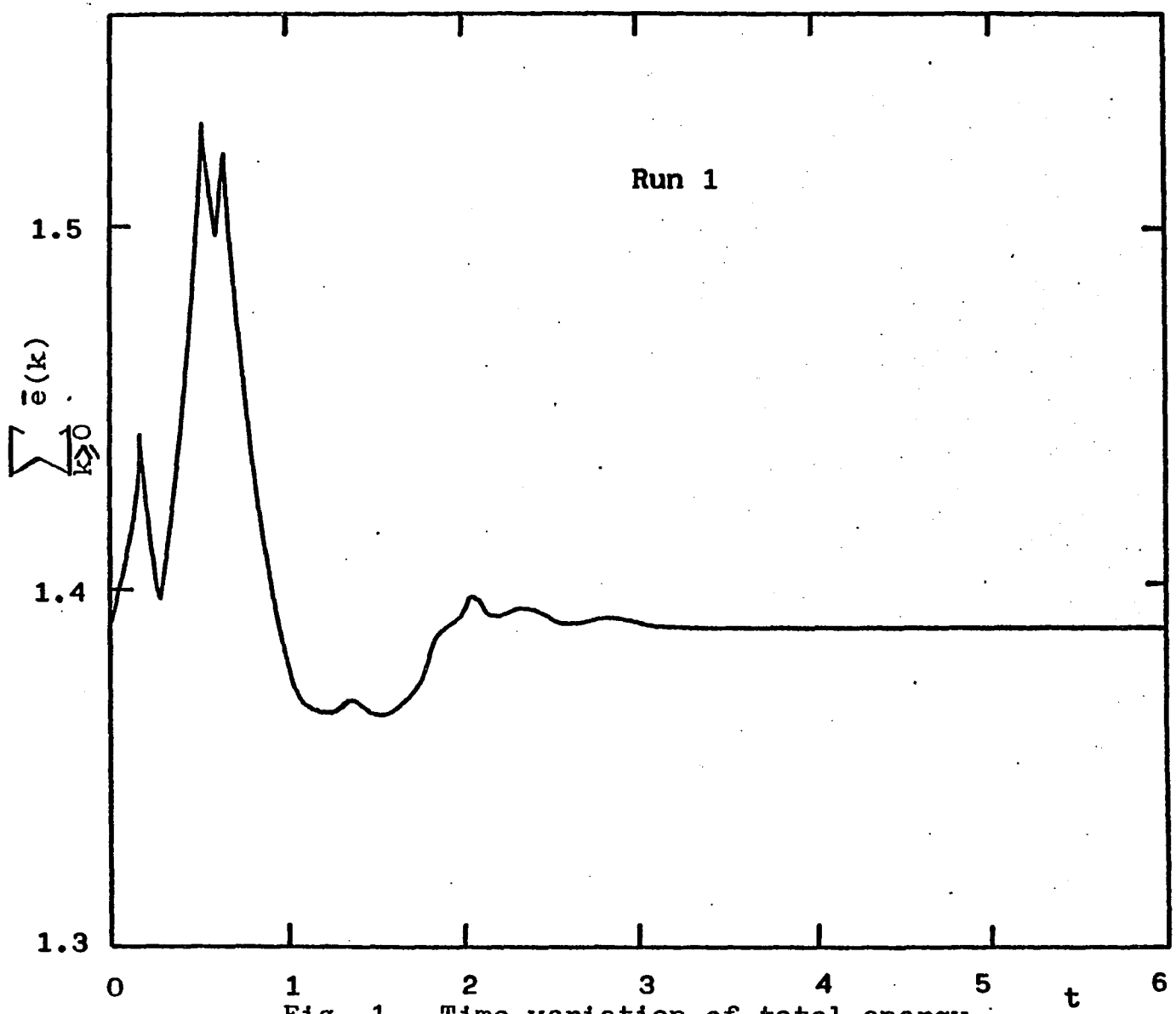

Fig. 1. Time variation of total energy

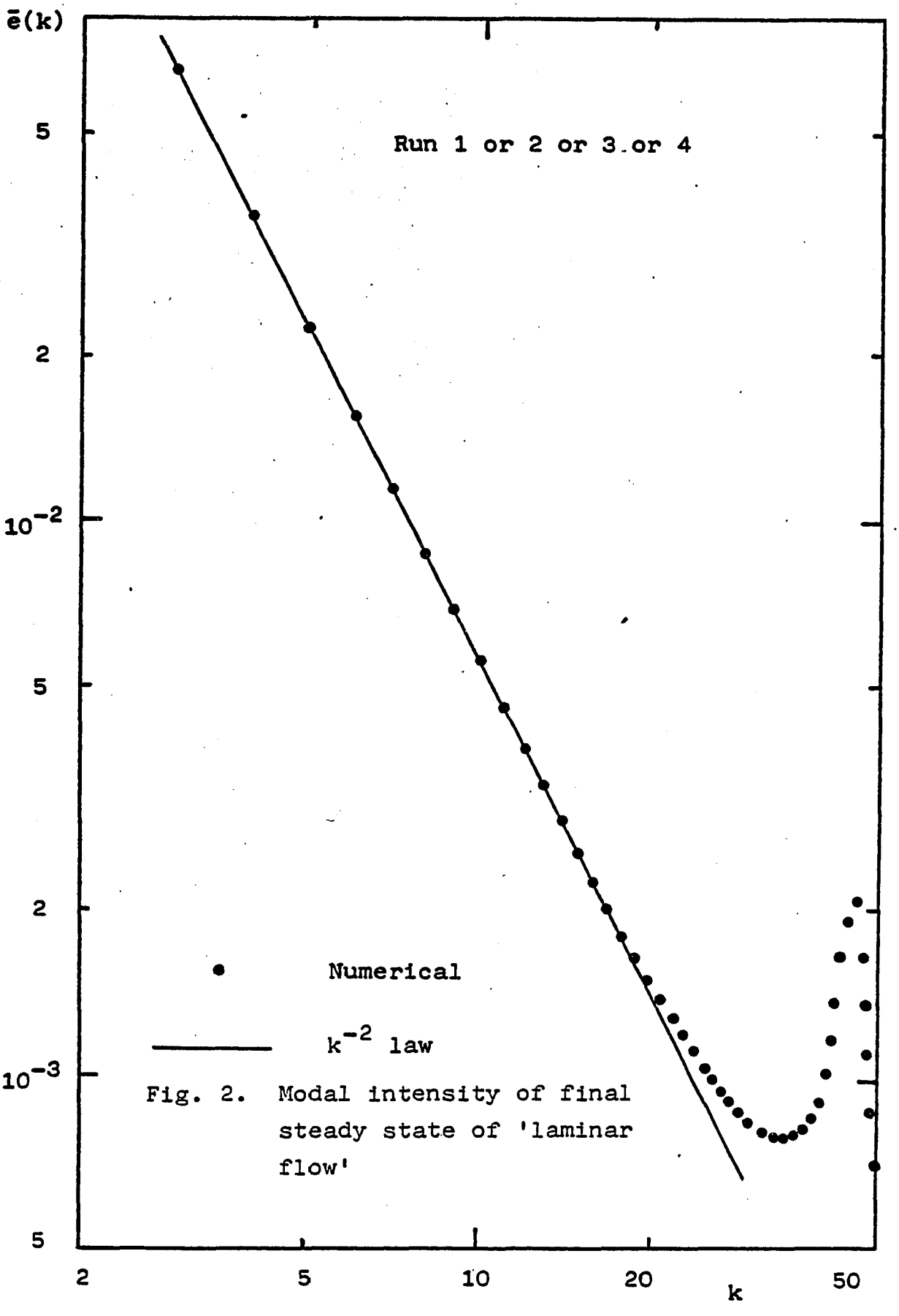

Fig. 2. Modal intensity of final steady state of 'laminar flow'

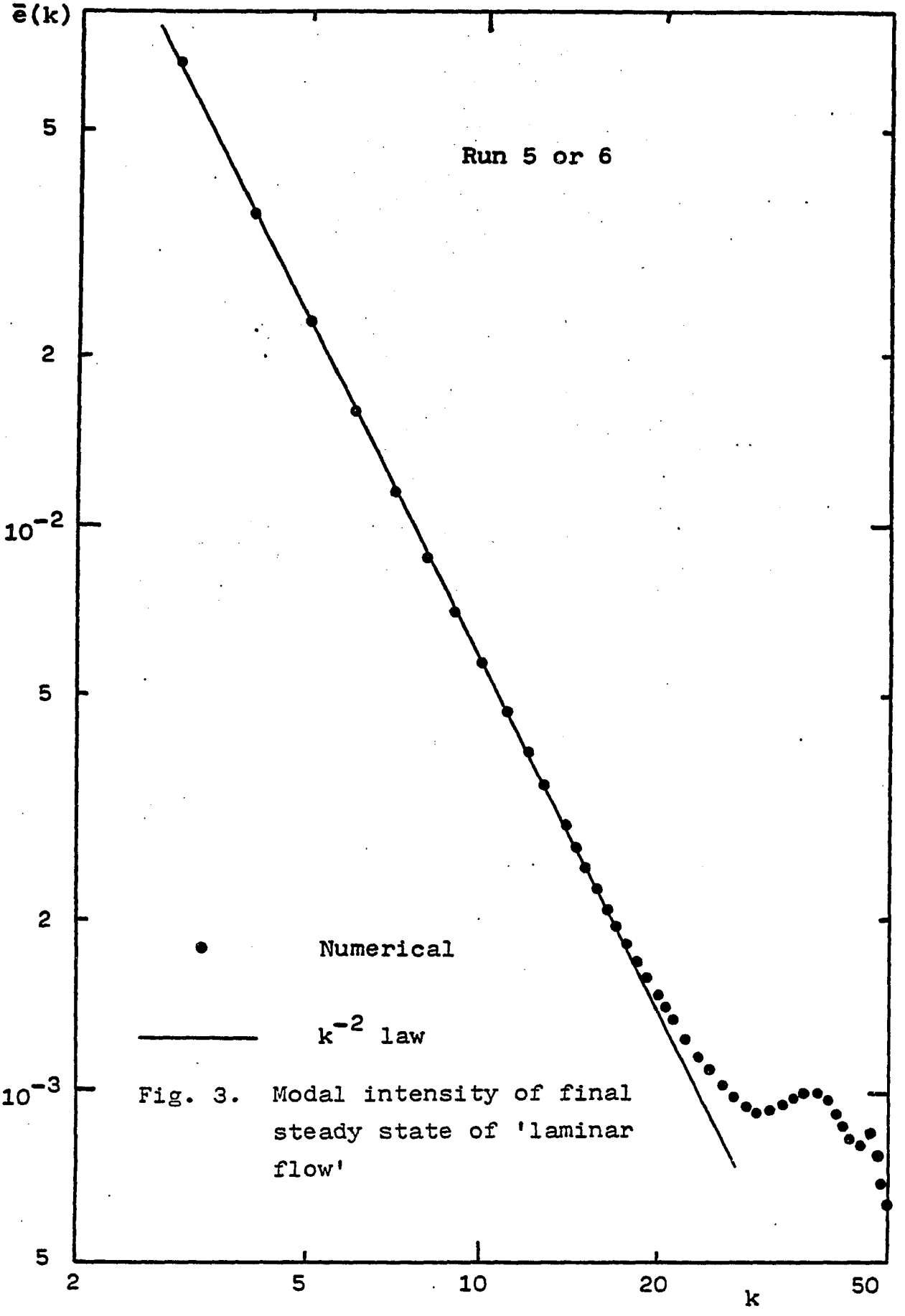

Fig. 3. Modal intensity of final steady state of 'laminar flow'

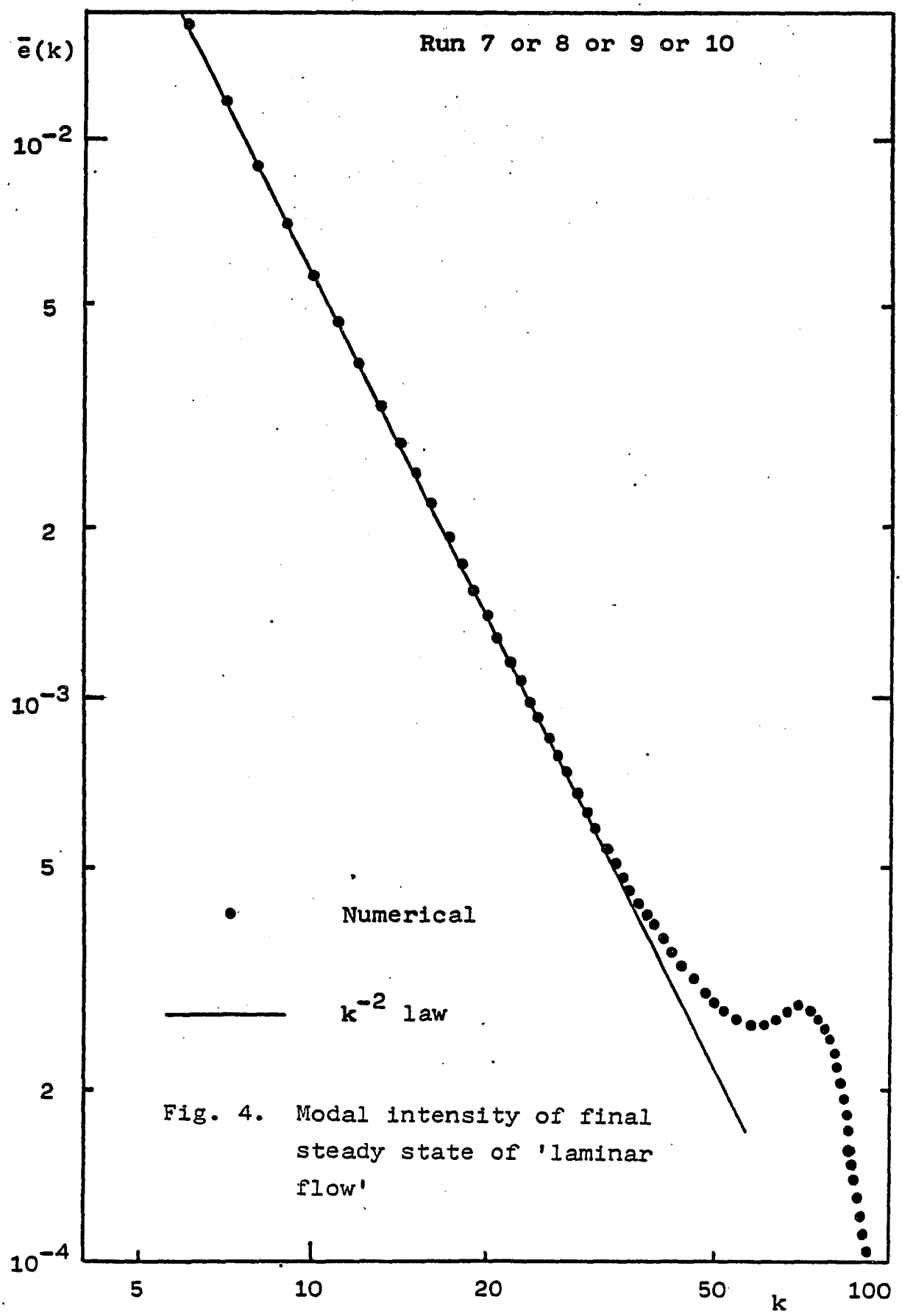

Fig. 4. Modal intensity of final steady state of 'laminar flow'

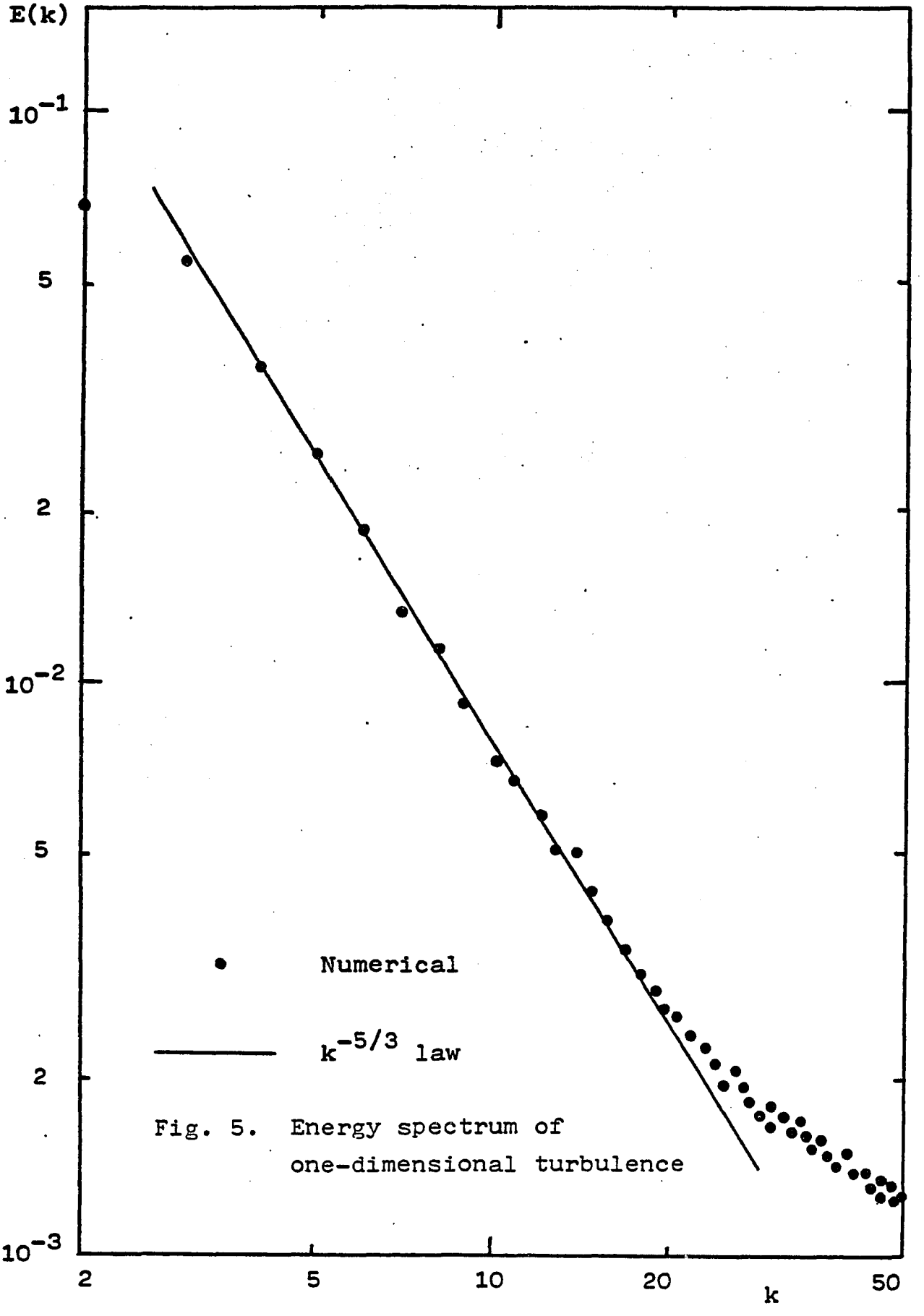

Fig. 5. Energy spectrum of one-dimensional turbulence

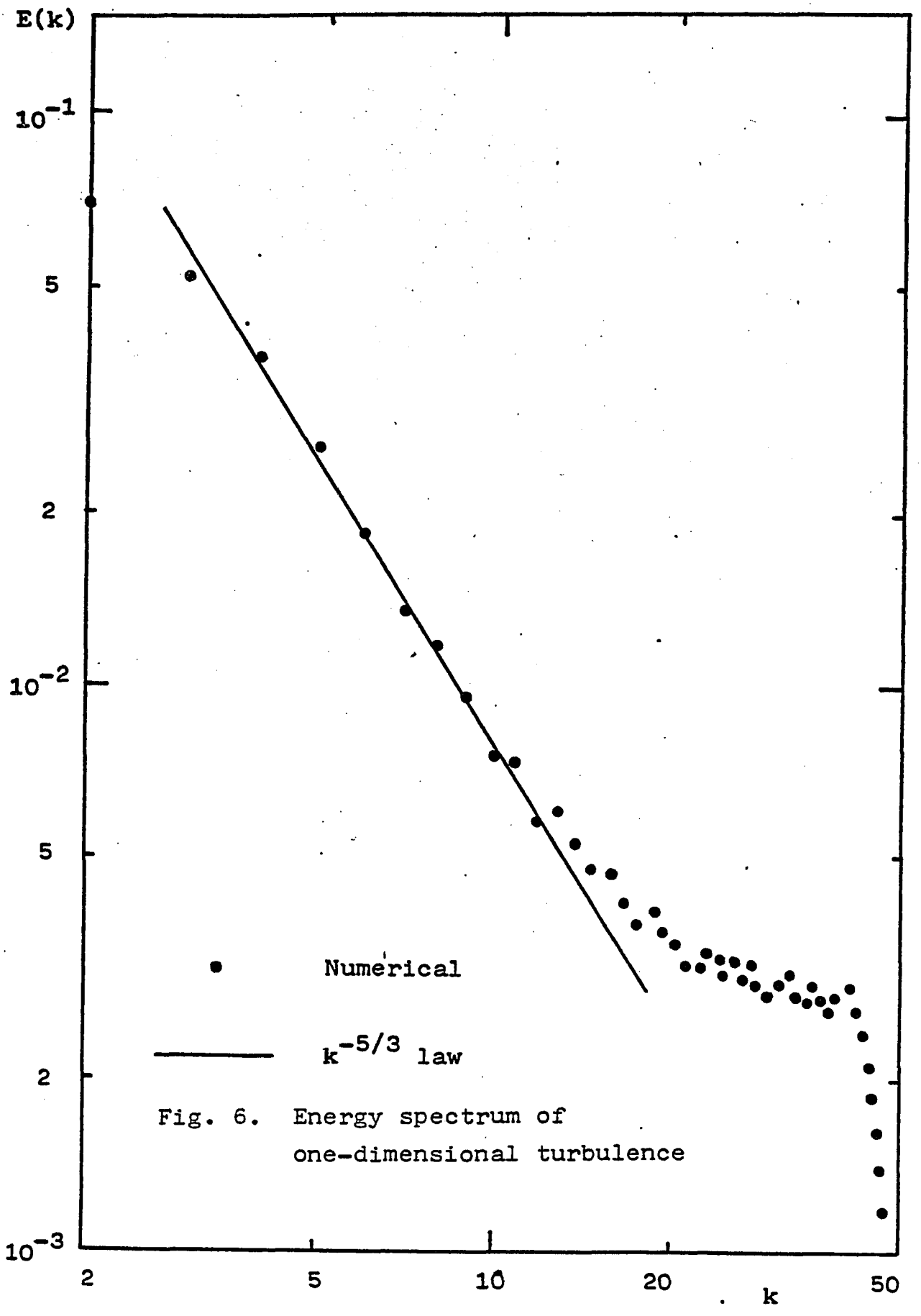

Fig. 6. Energy spectrum of one-dimensional turbulence

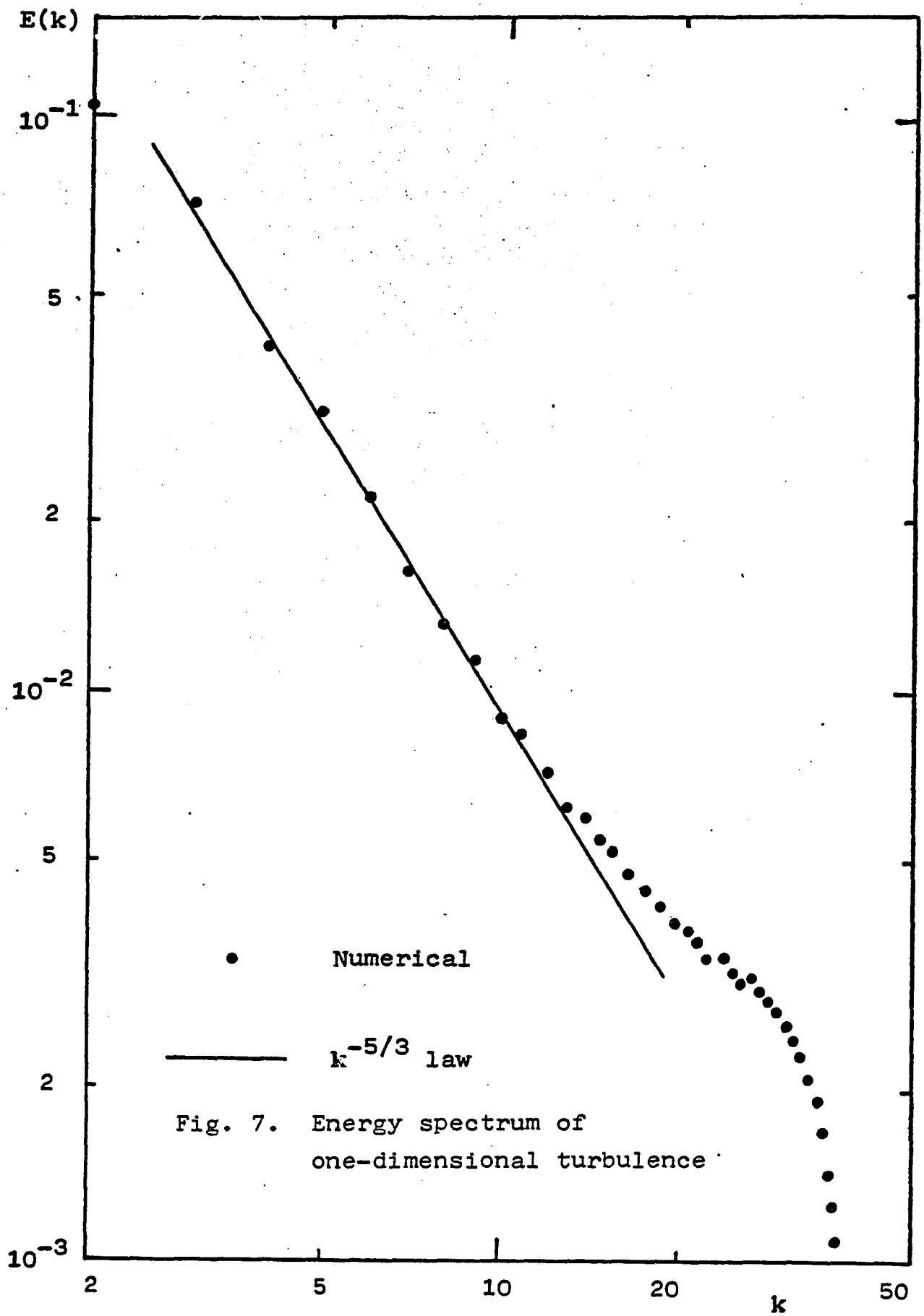

Fig. 7. Energy spectrum of one-dimensional turbulence

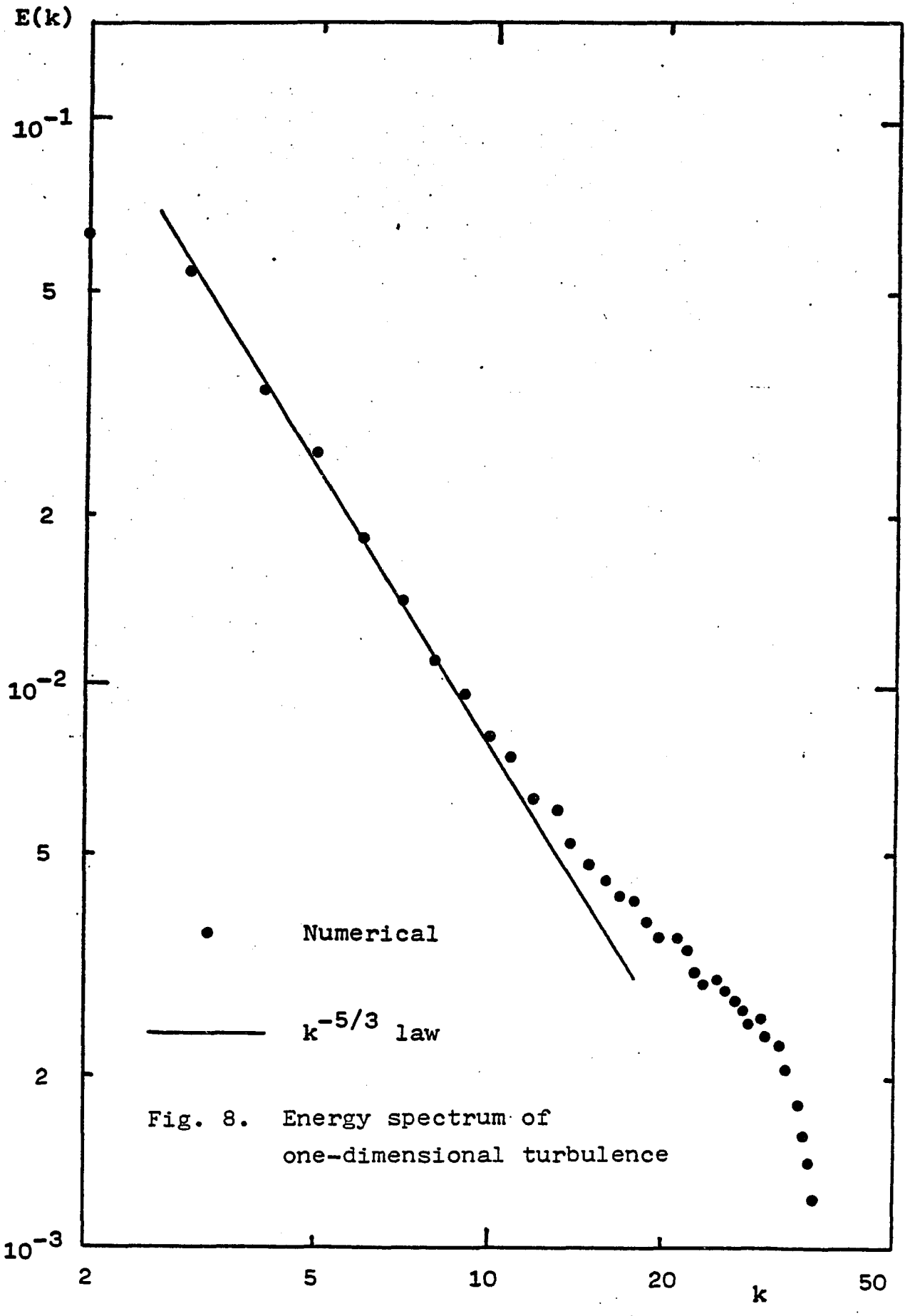

Fig. 8. Energy spectrum of one-dimensional turbulence

REFERENCES

1. D. C. Leslie, Developments in The Theory of Turbulence (Clarenden Press, Oxford, 1973)

2. J. O. Hinze, Turbulence (McGraw-Hill, New York, 1975), 2nd ed.

3. A. Monin and A. M. Yaglom, Statistical Fluid Mechanics of Turbulence (MIT, London, 1975)

4. S. A. Orzag, in Fluid Dynamics, edited by R. Balian and J. L. Peube (Gordon and Breach, New York, 1977)

5. Y. Ogura, J. Fluid Mech. 16, 33(1963)

6. R. H. Kraichnan, J. Fluid Mech. 5, 497(1959)

7. R. H. Kraichnan, Phys. Fluids 7, 1723(1964)

8. R. H. Kraichnan, Phys. Fluids 8, 575(1965)

9. R. H. Kraichnan, J. Fluid Mech. 47, 513(1971)

10. R. H. Kraichnan, J. Fluid Mech. 56, 287(1972)

11. R. H. Kraichnan, J. Fluid Mech. 83, 349(1977)

12. R. H. Kraichnan and J. R. Herring, J. Fluid Mech. 88, 355(1978)

13. J. R. Herring and R. H. Kraichnan, J. Fluid Mech. 91, 581(1979)

14. J. R. Herring and R. M. Kerr, J. Fluid Mech. 118, 205(1982)

15. S. F. Edwards, J. Fluid Mech. 18, 239(1964)

16. S. F. Edwards and W. D. McComb, J. Phys. A2, 157(1969)

17. J. R. Herring, Phys. Fluids 8, 2219(1965)

18. C. M. Tchen, C. R. Acad. Sci. Paris, 287B, 175(1978)

19. C. M. Tchen, A Kinetic Method of Turbulence (Preprint, 1982)

20. S. Chandrasekhar, Rev. Mod. Phys. 15, 1(1943)

21. H. Sagan, Introduction to The Calculation of Variatios (McGraw-Hill, New York, 1969)

22. A. Papoulis, Probability,Random Variables and Stochastic Processes (McGraw-Hill, New York, 1965)

23. J. M. Mendel, Discrete Technique of Parameter Estimation (Marcel-Dekker, New York, 1973)

24. C. H. Gibson and W. H. Schwarz, J. Fluid Mech. 16, 365(1963)

25. J. M. Burgers, Advances in Applied Mechanics. 1, 171(1948)

26. S. A. Orszag and G. S. Patterson, Phys. Rew. Lett. 28, 76(1972)

27. J. R. Herring, S. A. Orszag, R. H. Kraichnan and D. G. Fox, J. Fluid. Mech. 66, 417(1974)

28. B. Fornberg, J. Comput. Phys. 25, 1(1977)

29. E. Hopf, Commun. Pure Appl. Math. 3, 20(1950)

30. J. D. Cole, Quart. Appl. Math. 9, 1225(1951)

31. D. T. Jeng, R. Foerster, S. Haaland and W. C. Meecham, Phys. Fluids 9, 2114(1966)

32. I. Hosokawa and Yamamoto, Phys. Fluids 7, 1683(1970)

33. T. Tasumi and S. Kida, J. Fluid Mech. 55, 659(1972)

34. S. Kida, J. Fluid Mech. 93, 337(1979)

35. D. T. Jeng, Phys. Fluids 12, 2006(1969)

36. S. Kida and M. Sugihara, J. Phys. Soc. Jan. 50, 1785(1981)

37. R. H. Kraichnan, Phys. Fluids 11, 265(1968)

38. Y. A. Shreider, Method of Statistical Testing (Elserier Publishing Co., New York, 1964)

39. S. Chapman and T. G. Cowing, The Mathematical Theory of Non-umiform Gases (Cambridge U.P., 1952)

40. J. Qian, Acta. Phys. Sin. 20, 1061(1964)

41. A. N. Kolmogorov, C. R. Acad. Sci. USSR 30, 301(1941)